Received: 30 April 2021 | Revised: 9 September 1999 | Accepted: 2 December 2021

DOI: 10.1002/mbo3.1258

ORIGINAL ARTICLE

MicrobiologyOpen Open Access WILEY

Novel nitrite reductase domain structure suggests a chimeric denitrification repertoire in the phylum Chloroflexi

Sarah L. Schwartz[1,2] | Lily Momper[2,3] | Luiz Thiberio Rangel[2] | Cara Magnabosco[4] | Jan P. Amend[5,6] | Gregory P. Fournier[2]

[1]Microbiology Graduate Program, Massachusetts Institute of Technology, Cambridge, Massachusetts, USA

[2]Department of Earth, Atmospheric, and Planetary Sciences, Massachusetts Institute of Technology, Cambridge, Massachusetts, USA

[3]Exponent Inc., Pasadena, California, USA

[4]Department of Earth Sciences, ETH Zurich, Zurich, Switzerland

[5]Department of Earth Sciences, University of Southern California, Los Angeles, California, USA

[6]Department of Biological Sciences, University of Southern California, Los Angeles, California, USA

Correspondence

Sarah L. Schwartz, Microbiology Graduate Program, Massachusetts Institute of Technology, 77 Massachusetts Avenue, 54-1027, Cambridge, MA 02139, USA.
Email: sschwart@mit.edu

Funding information

Simons Collaboration on Origins of Life, Grant/Award Number: 339603; National Defense Science and Engineering Graduate Fellowship

Abstract

Denitrification plays a central role in the global nitrogen cycle, reducing and removing nitrogen from marine and terrestrial ecosystems. The flux of nitrogen species through this pathway has a widespread impact, affecting ecological carrying capacity, agriculture, and climate. Nitrite reductase (Nir) and nitric oxide reductase (NOR) are the two central enzymes in this pathway. Here we present a previously unreported Nir domain architecture in members of phylum Chloroflexi. Phylogenetic analyses of protein domains within Nir indicate that an ancestral horizontal transfer and fusion event produced this chimeric domain architecture. We also identify an expanded genomic diversity of a rarely reported NOR subtype, eNOR. Together, these results suggest a greater diversity of denitrification enzyme arrangements exist than have been previously reported.

KEYWORDS

Chloroflexi, cytochrome, denitrification, nitric-oxide reductase, nitrite reductase, phylogeny

1 | INTRODUCTION

Microbial denitrification is a key pathway in global nitrogen cycling and has been studied extensively for its role in fixed nitrogen loss and as a source of potent greenhouse gases (Decleyre et al., 2016; Zumft, 1997). Diverse bacteria are capable of denitrification, often facultatively using nitrate or nitrite as an alternative electron acceptor in oxygen-limited zones. Several diverse microorganisms have the genomic capacity to perform complete denitrification (Figure 1), reducing nitrate to dinitrogen gas (Canfield et al., 2010; Philippot, 2002).

Denitrification has been widely reported in various taxa (Philippot, 2002; Zumft, 1997), and the utility of the pathway is underscored by the diversity of key constituent enzymes. The canonical denitrification enzyme is dissimilatory nitrite reductase, Nir, which reduces nitrite to nitric oxide (NO). Nir functionality is

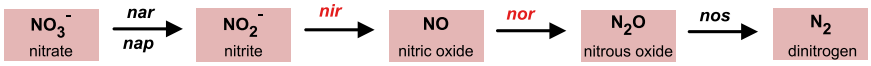

FIGURE 1 Denitrification. Complete denitrification transforms nitrate into dinitrogen gas. Respiratory nitrate reductase gene (*nar*) and periplasmic nitrate reductase (*nap*) genes are distributed in non-denitrifying organisms. Nitrite reductase (Nir) is considered the canonical first enzyme of denitrification (Graf et al., 2014), followed by nitric oxide reductase (NOR) and nitrous oxide reductase (Nos)

found in two distinct enzymes—the copper-based nitrite reductase NirK, and the cytochrome-type reductase NirS (Braker et al., 2000; Decleyre et al., 2016; Priemé et al., 2002). NirS reduces nitrite via cytochrome *cd1*, a dimer of subunits each containing heme *c* and heme *d1*; in canonical denitrification, as observed in *Pseudomonas aeruginosa*, cytochrome *cd1* catalyzes the oxidation of a colocalized cytochrome c551 to reduce nitrite to NO at the heme *d1* site (Philippot, 2002; Zumft, 1997). The *nirS* gene has been reported as a constituent of a larger gene cluster containing genes such as *nirM* and *nirF*, which encode biosynthetic proteins for the cytochrome *c*551 and heme d_1, respectively, and the nitrite transporter *nirC* (Kawasaki et al., 1997; Philippot, 2002).

The next step in the pathway—the reduction of NO to nitrous oxide—is catalyzed by nitric oxide reductases (NORs). Most bacterial NORs are homologous and closely related to one another, and to oxygen reductases in the heme–copper oxygen reductase superfamily (Hemp & Gennis, 2008). The most widely studied NOR enzymes are cytochrome-type nitric oxide reductases (cNOR) and quinol-dependent nitric oxide reductases (qNOR) (Graf et al., 2014; Hemp & Gennis, 2008; Hendriks et al., 2000), distinguished by their respective electron donors. Enzymes in the cNOR subfamily have two subunits—one catalytic site and one heme-containing electron shuttle that accepts electrons from cytochrome *c*—while qNOR family enzymes' single, fused subunit accepts electrons from membrane-bound quinol groups (Hemp & Gennis, 2008). Rarer, alternative NOR enzymes, including sNOR, gNOR, and eNOR, have been more recently identified and characterized in limited members of the Proteobacteria, Firmicutes, Archaea, and Chloroflexi (Hemp & Gennis, 2008; Hemp et al., 2015; Sievert et al., 2008; Stein et al., 2007). Like cNOR, these enzymes are predicted to have a two-subunit structure, but the second subunit in these NORs contains a cupredoxin instead of heme *c* fold (Hemp & Gennis, 2008).

Many bacteria contain genes encoding only one or a partial subset of the four denitrification steps. Such organisms may perform partial denitrification, while others may use one of these enzymes for nondenitrifying functions (Graf et al., 2014; Hendriks et al., 2000; Roco et al., 2017; Sanford et al., 2012). In partial denitrifiers, the co-occurrence of denitrification pathway genes appears to vary across different taxa and environments (Graf et al., 2014). Some of this variation may be constrained by the chemistry of certain intermediates. For example, nitric oxide (NO), the product of NirS and NirK, is highly cytotoxic. Both Nir types are periplasmic, and so cells require a means of effluxing or detoxifying NO before it accumulates to lethal levels. Denitrifiers are thought to immediately reduce NO to nitrous oxide (N_2O) to avoid injury, using membrane-bound NOR enzymes (Hendriks et al., 2000). Perhaps, for this reason, it is rare to find genomes that contain *nir* but not *nor*, while organisms showing the inverse—the presence of a *nor* gene but not a *nir* gene—are far more common (Graf et al., 2014; Hendriks et al., 2000). While cNORs are only found in denitrifying microbes, other types of NOR—for example, quinol-dependent qNOR—are found in nondenitrifiers and can presumably detoxify environmental NO (Hendriks et al., 2000). Beyond NORs, alternative pathways to NO detoxification are possible, including alternative enzymes such as cytochrome *c* oxidase (Blomberg & Ädelroth, 2018) or oxidoreductase (Gardner et al., 2002), flavorubredoxin (Gardner et al., 2002), or flavohemoglobins (Sánchez et al., 2011).

While denitrification has been most widely studied and observed in Proteobacteria, the process has also been identified in other phyla, including Chloroflexi. Chloroflexi are ecologically and physiologically diverse, and often key players in oxygen-, nutrient-, and light-limited environments, including anaerobic sludge and subsurface sediments (Hug et al., 2013; Ward, Hemp et al., 2018). Previous surveys have indicated the presence of diverse nitrite reductases in Chloroflexi; members of order Anaerolineales and classes Chloroflexia and Thermomicrobia may have the capacity for nitrite reduction via the copper-type NirK (Decleyre et al., 2016; Hug et al., 2013; Wei et al., 2015). However, recent studies indicate that certain Chloroflexi—including members of Anaerolineales—may possess *nirS* instead of *nirK* (Hemp et al., 2015; Ward, McGlynn et al., 2018), and may also harbor a divergent variant of *nor* previously reported in members of Archaea (Hemp & Gennis, 2008; Hemp et al., 2015). These findings suggest that the evolution and/or biochemistry of denitrification may be unusual for this subset of bacteria, and informative for a broader understanding of microbial denitrification metabolisms and their origin.

2 | EXPERIMENTAL PROCEDURES

2.1 | Genome sampling and assembly

Collection of all fluid samples and total genomic DNA extractions from those fluids, as well as corresponding physical and geochemical data, have been described previously (Heard et al., 2017; Lau et al., 2014, 2016; Magnabosco et al., 2016; Momper & Jungbluth, 2017; Momper & Kiel Reese, 2017; Osburn et al., 2014). All metagenome-assembled genomes (MAGs) from North America and Africa were reconstructed according to the methods used in Momper and Jungbluth (2017). MAG identifiers

and sources are listed in Table A5. Completeness was calculated using the composite values from five widely accepted core essential gene metrics. Duplicate copies of any of these single-copy marker genes were interpreted as a measure of contamination (Alneberg et al., 2014; Campbell et al., 2013; Creevey et al., 2011; Dupont et al., 2012; Wu & Scott, 2012). Individual genomes were then submitted for gene calling and annotations through the DOE Joint Genome Institute IMG-ER (Integrated Microbial Genomes expert review) pipeline (Huntemann et al., 2015; Markowitz et al., 2008). For quality control purposes, the genes flanking every denitrification gene presented in this study were individually searched on the National Center for Biotechnology Information's (NCBI) RefSeq database using the BLASTp algorithm, confirming that top hits for all flanking genes were also to Chloroflexi. This step ensured that the nitrogen transforming genes of interest presented here were not simply on scaffolds that were incorrectly binned into a putative Chloroflexi genome.

2.2 | Genetic database construction and sequence sampling

Sequences for *nirS* and *eNOR* genes from Sanford Underground Research Facility (SURF) MAG 42 (see Table A5) were used as queries to BLAST (Camacho et al., 2009) three genomic repositories:

1. Genome databases constructed for 21 Chloroflexi genomes assembled from deep-subsurface MAG data (Jungbluth et al., 2017; Momper & Jungbluth, 2017; Table A5).
2. Genome databases constructed for 86 genomes from recent MAG assembled sludge bioreactor genomes (Parks et al., 2017; Table A6).
3. The full NCBI nonredundant protein database (as of September 25, 2019; Agarwala et al., 2018).

Additionally, putative environmental homologs were evaluated using protein sequence data from SURF MAG 42 to query NCBI's nonredundant environmental metagenomic sequence database (env-nr, as of June 2020; Agarwala et al., 2018). Hits from all databases were combined and assessed for quality; hits with $E \leq 1 \times 10^{-10}$ were included for initial analyses. To capture diversity while limiting imprecision and biased sampling of overrepresented groups (e.g., Proteobacteria), hits were subsampled to the genus level, except for members of the Chloroflexi (to fully capture the taxonomic distribution of the novel gene variant). One additional, divergent multispecies hit was allowed per genus. The genus-level filter was also removed for C1, where non-Chloroflexi hits were severely limited (see below). Duplicate sequences (from strains with multiple genome entries or in multiple databases surveyed) were removed. Expanded database hits and filtering data are available as Supporting Information Data Files at https://doi.org/10.6084/m9.figshare.14515554.v2.

2.3 | Sequence alignment

Putative homologous protein sequences were aligned with MAFFT, using autoparameterization (Nakamura et al., 2018), and visualized in Jalview (A. M. Waterhouse et al., 2009). Alignments were manually curated; partial sequences with substantial missing regions or anomalous insertions in conserved regions of the protein were removed to avoid confounding phylogenetic analyses and evolutionary model selection. Protein sequence alignments were trimmed to the length of individual domains identified by NCBI's Conserved Domains Database (CDD). Each domain was then realigned.

2.4 | eNOR

A preliminary alignment for the *eNOR* gene showed a poorly conserved region near the C-terminal end of the open reading frame (ORF); to improve accuracy and avoid misalignment, this region was manually removed, and the remaining sequences were realigned before tree construction. Two sequences (Actinobacteria bacterium RBG_16_68_12, OFW73639.1, and *Thermus* WP_015717644.1) with missing N-terminal regions and three sequences (Chloroflexi bacterium, RME47896.1; Rhodocyclaceae bacterium UTPRO2, OQY7467.1; and *Rhodothermus profundi*, WP_072715415.1) with missing C-terminal regions were included in the final alignment; the placement of these sequences is therefore based upon fewer alignment sites than other taxa. All retain key active site residues and show no clear evidence of long-branch attraction artifacts in the tree.

2.5 | C1

An initial alignment for the C1 domain showed a poorly conserved N-terminal region. To improve accuracy, this region was manually removed, and the remaining sequences realigned before tree construction.

2.6 | NirS

Because the NirS domain had a C-terminal placement in the ORF across hits, C-terminal sites extending beyond the identified NirS domain were included in the trimmed alignment.

2.7 | Rooting and outgroup identification

2.7.1 | eNOR

Ingroup *eNOR* subunit I sequences were identified by the presence of a conserved Gln residue in alignment position 323. This site distinguishes eNOR not only from other NORs but also from members of the oxygen reductase superfamily, which have a conserved Tyr in this

site that plays a role in cofactor crosslinking (Hemp & Gennis, 2008; Table A4). Outgroup sequences (oxygen reductase superfamily or other divergent NORs) were subsampled to a single taxon representative per major subgroup observed in a preliminary tree. Retained outgroup sequences CCQ74688.1, WP_100277903.1, WP_097280063.1, WP_089728124.1, RLC59399.1, and WP_083704903.1 are annotated as uncharacterized domains. The remaining sequences were realigned before tree construction and manually rooted on the branch leading to the outgroup.

2.7.2 | C1

Due to a paucity of initial hits (17 total genera), the genus-level filter was removed for all phyla to increase the resolution of the domain phylogeny. A preliminary tree (Figure A8) was expanded to identify outgroup sequences by including hits with $E \leq 10^{-4}$. The resulting tree was rooted using minimal ancestor deviation (MAD) rooting (Tria et al., 2017).

2.7.3 | C2 and NirS

Sequences were rooted using MAD rooting (Tria et al., 2017).

2.8 | Tree construction

Maximum-likelihood trees were constructed using IQ-Tree (Nguyen et al., 2015), under the optimal model defined by the ModelFinder (-MFP) command (Kalyaanamoorthy et al., 2017; Table A7). Ultrafast bootstraps and approximate likelihood ratio tests were performed using IQ-Tree's ultrafast bootstrap and Sh-aLRT parameters (Hoang et al., 2018; Minh et al., 2013). Full domain and gene sequences, sequence alignments, and raw treefiles are available as Supporting Information Data Files at https://doi.org/10.6084/m9.figshare.14515554.v2.

2.9 | Gene and enzyme structural analysis

FIND (Murali et al., 2019) was used to identify structural features and conserved denitrification pathway genes in deep subsurface genomes. Putative domains within denitrification gene ORFs were identified and compared across genomes using BLAST and NCBI's CDD (S. Lu et al., 2020; Marchler-Bauer et al., 2015) and EMBL InterPro (Mitchell et al., 2019). C1 from SURF MAG 42 was classified by CDD as COG4654 ($e = 6.4 \times 10^{-4}$) and by hmmscan (Potter et al., 2018) as cytochrome *c* superfamily (accession 46626) hit ($e = 1.6 \times 10^{-5}$). C1 did not show a strong pfam match in hmmscan; the closest match was PF13442.8 (independent $e = 0.18$). C2 from SURF MAG 42 was classified by CDD as COG2010 ($e = 5.31 \times 10^{-9}$), and included an annotated region classified as pfam 13442 ($e = 4.06 \times 10^{-7}$); C2 was identified in hmmscan as a cytochrome *c* superfamily (accession 46626) hit ($e = 1.2 \times 10^{-17}$), with a pfam match to PF13442.8 (independent $e = 2.8 \times 10^{-10}$). While clearly homologous, the C1 and C2 families appear distantly related and do not appear within the other's data set of closely related sequences (see above). Gene neighborhoods were visualized using Gene Graphics (Harrison et al., 2018), using a 20,000 base pair region. Gene and domains identified in each neighborhood were sourced and cross-referenced with NCBI's RefSeq and CDD (Marchler-Bauer et al., 2015; O'Leary et al., 2016). Existing enzyme structures for canonical denitrification genes were downloaded from the RCSB Protein Data Bank (Berman et al., 2000). Anaerolineales-type enzyme structures were predicted using SWISS-MODEL (A. Waterhouse et al., 2018). All enzyme structures were visualized and analyzed in PyMOL (The PyMOL Molecular Graphics System, Version 2.0, Schrödinger, LLC). SWISS-MODEL outputs are available at https://doi.org/10.6084/m9.figshare.14515554.v2.

3 | RESULTS

To investigate divergent denitrification genes in Chloroflexi, we performed a comprehensive analysis of denitrification homologs in over 100 recently sequenced Chloroflexi MAGs, as well as previously available genomes and metagenomes from the NCBI protein databases. Domains of interest were initially identified in SURF MAG 42, an Anaerolineales bacterium sampled in the SURF, a former gold mine in South Dakota (Momper & Jungbluth, 2017).

3.1 | Apparent chimeric fusion in Chloroflexi NirS

Domain analysis of the Anaerolineales-type nitrite reductase ORF from SURF MAG 42 indicated three putative functional regions of interest: one cytochrome-type NirS domain and two cytochrome *c* superfamily domains (Figure 2).

The first cytochrome domain (C1) in the Anaerolineales-type ORF was identified by NCBI's CDD (S. Lu et al., 2020; Marchler-Bauer et al., 2015) as a cytochrome c551/552. The second cytochrome domain (C2) was predicted with high specificity as a cytochrome *c* mono- and diheme variant. C2 included a region predicted as a cbb3-type cytochrome *c* oxidase subunit III; such subunits frequently contain two cytochromes (Bertini et al., 2006).

Gene neighborhood analyses indicated that the MAG-derived nitrite reductase ORF displays a very different local genomic environment as compared with a canonical nitrite reductase neighborhood in *P. aeruginosa PAO1* (Figure 3). In *P. aeruginosa*, *nirS* (NCBI reference sequence NP_249210.1; O'Leary et al., 2016) co-occurs with other genes in the *nir* operon and is closely adjacent to genes encoding a cNOR. This arrangement places nitrite reduction in *cis* with NO reduction, the next step of canonical denitrification. In the Chloroflexi MAG, no other denitrification genes appear within a 20,000 base pair neighborhood for the C1-C2-NirS nitrite reductase.

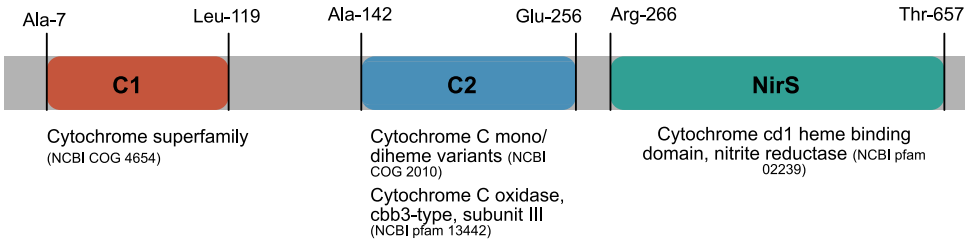

FIGURE 2 Open reading frame domain map. Conserved domain analysis of SURF MAG 42 Chloroflexi nitrite reductase (GenBank RJP53747.1) indicates the presence of two distinct cytochrome superfamily domains and a C-terminal nitrite reductase domain. MAG, metagenome-assembled genome; SURF, Sanford Underground Research Facility

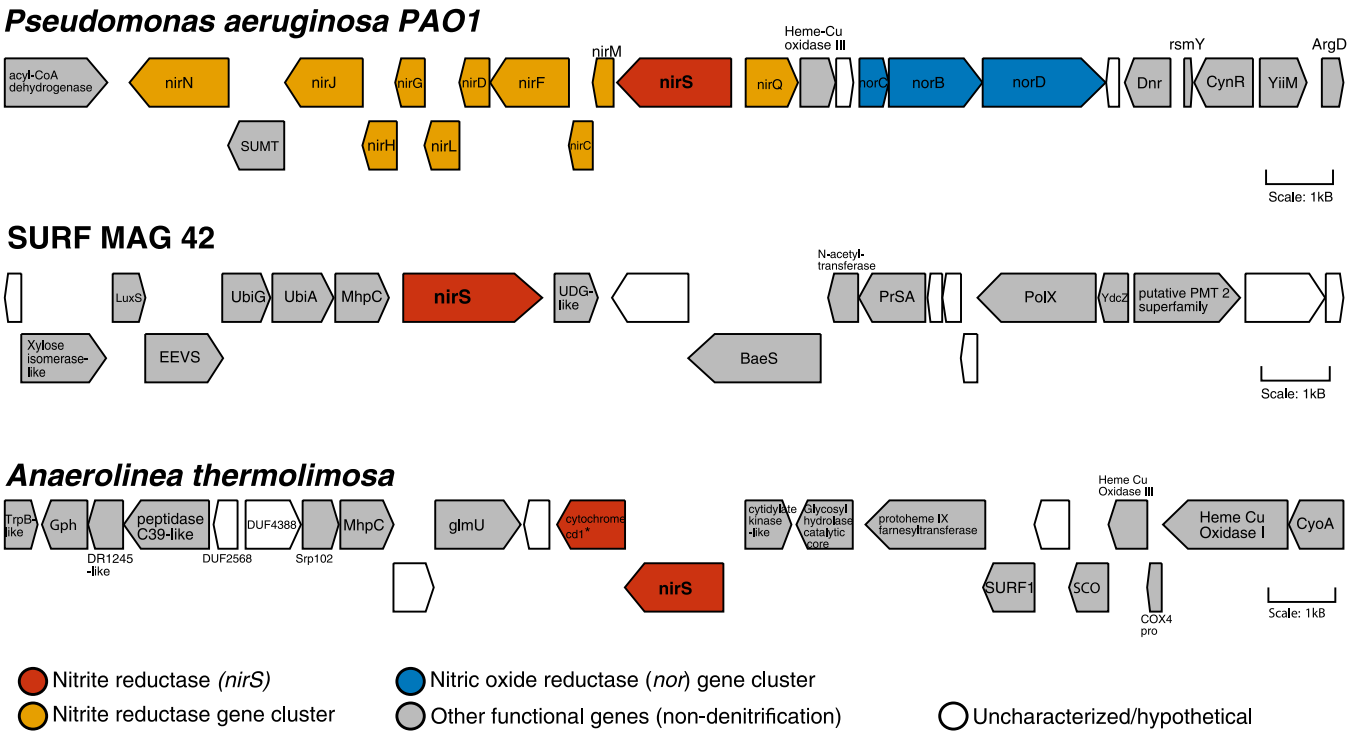

*Cytochrome cd1 in *A. thermolimosa* contains an isolated NirS cytochrome D1 heme domain (see Table S1).

FIGURE 3 NirS gene neighborhood in SURF MAG 42 versus *Pseudomonas aeruginosa*. Gene neighborhood analyses of the 20,000 base pair region surrounding *nirS* differ markedly between *P. aeruginosa PAO1* (GenBank reference sequence NP_249210.1, top) and two Chloroflexi genomes containing the C1-C2-NirS gene: SURF MAG 42 (center) and *Anaerolinea thermolimosa* (bottom). While the *P. aeruginosa* nitrite reductase occurs as part of a larger *nir* operon, and in close proximity to nitric oxide reductase genes, the *nirS* ORF neighborhoods in SURF MAG 42 and *A. thermolimosa* do not appear to contain other denitrification-specific genes. Detailed descriptions of ORF/gene families and functions can be found in Table A1. MAG, metagenome-assembled genome; ORF, open reading frame; SURF, Sanford Underground Research Facility

A similar pattern is observed for a homologous C1-C2-NirS nitrite reductase gene identified in the Chloroflexi *Anaerolinea thermolimosa* (Matsuura et al., 2015); the *A. thermolimosa* neighborhood also shows no evidence of other denitrification genes in the immediate vicinity of the novel NirS, though it does contain some ORFs with predicted functionality similar to those in the SURF MAG 42 neighborhood (Figure 3). Full descriptions of all gene abbreviations are provided in Table A1. Analyses of additional selected C1-C2-NirS ORF neighborhoods within other Chloroflexi reveal diverse genetic assemblages also dissimilar to the canonical *Pseudomonas* operon (Figure A1, Table A2).

Conserved domain analysis of NirS homologs in this study suggests that while the C2 and NirS functional domains frequently co-occur in nitrite reductases, the inclusion of C1 in the ORF appears extremely rare and limited to Chloroflexi. A lineage-specific fusion of multiple gene domains could explain this novel C1-C2-NirS arrangement. Different evolutionary histories among the domain subunits within Chloroflexi would provide evidence for an ancestral horizontal acquisition and fusion event.

To compare the evolutionary histories of each domain in the enzyme ORF, and to determine if the different domains have different ancestry, maximum-likelihood domain trees were

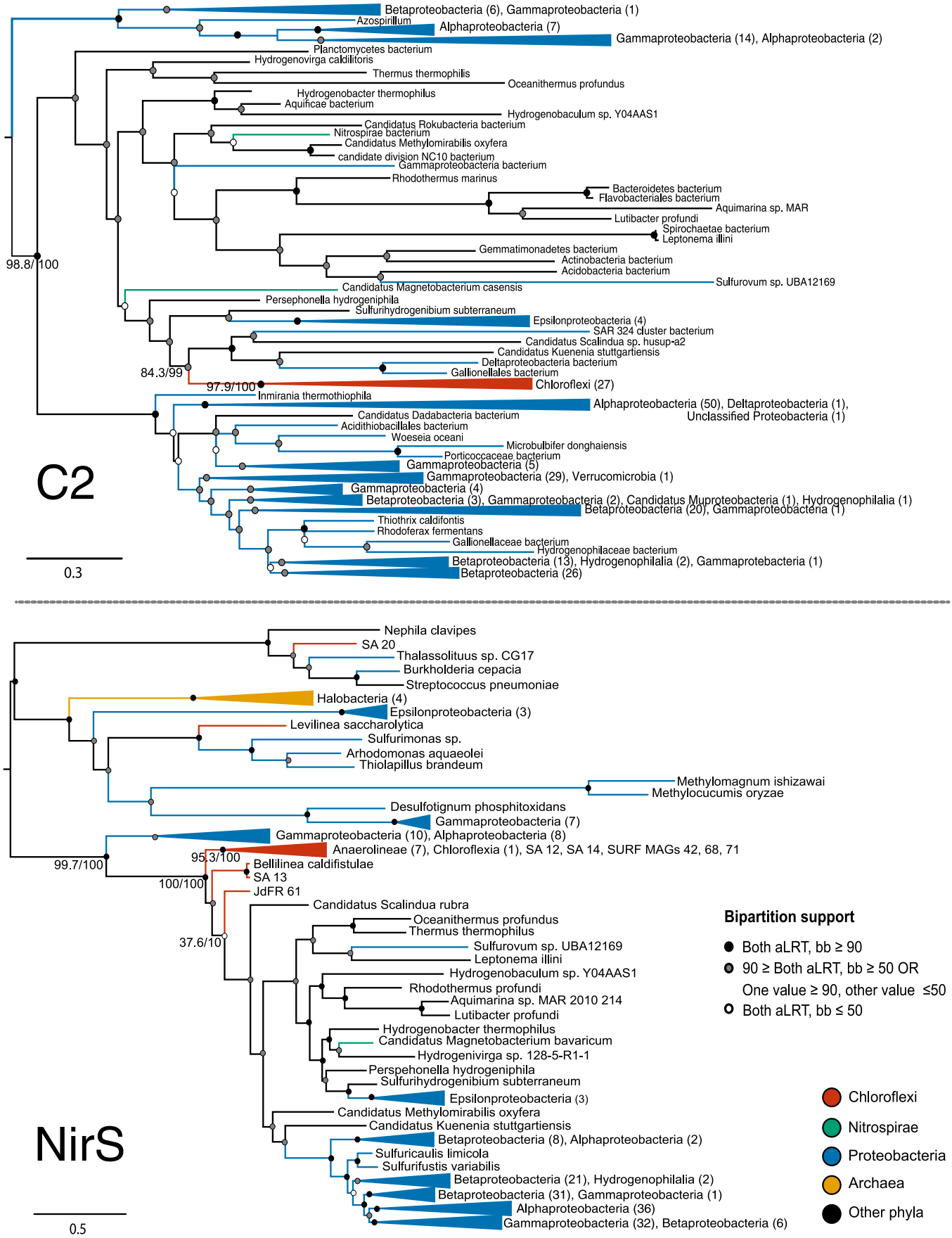

FIGURE 4 (See caption on next page)

reconstructed independently for C1, C2, and the NirS-specific domain (see Methods).

Domain phylogenies indicate similar taxonomic distributions for the C2 and NirS domains (Figure 4). The relative placement of Chloroflexi sequences varies slightly between domain trees: For the C2 domain tree, Chloroflexi sequences are monophyletic within a larger clade comprising polyphyletic sequences including members of the Aquificae, Bacteroidetes, Epsilonproteobacteria, and Spirochaetia; this clade places sister to a large group dominated by Alpha-, Beta-, and Gammaproteobacteria (expanded tree available as Figure A2). In the NirS domain tree, Chloroflexi place basally in a clade shared with both polyphyletic sequences and the large radiation of Proteobacterial sequences (expanded tree available as Figure A3).

C2 and NirS domain trees reconstructed exclusively from ORFs containing both domains produce similar topologies, albeit with slightly different placement of these major groups of taxa (Figures A4 and A5). Interestingly, the subsampling inverts the placements of the Chloroflexi with respect to the largest Proteobacterial group, as compared with the unsampled trees. This change suggests that sampling and phylogenetic noise are likely responsible for the observed differences in the C2 and NirS domain phylogenies. Additionally, there are notable differences in placement among subclades within the Proteobacteria, and low bipartition support for these subclades for the C2 tree, suggesting that patterns unrelated to Chloroflexi evolution may be polarizing the relative placements of groups in the tree. This lack of robustness caused by alternative sampling, combined with poor support values within the polyphyletic clade or between this clade and the Proteobacteria, suggests that the differences in tree topology may be artifactual, and not reflective of gene reticulation events.

The inferred phylogeny for C1 shows a much different evolutionary history than the other two domains (Figure 5). In contrast to the domain trees for C2 or NirS, the C1 tree shows sequences from Nitrospirae and Nitrospinae grouping together within a large clade of Chloroflexi C1 domains. Additional Chloroflexi sequences group with a small number of more distantly related Proteobacteria. However, the placement and taxonomic representation of Proteobacteria in the C1 tree is different from that seen in the other domain trees.

The majority of ORFs represented in the C1 domain tree contain the C1 domain homolog either as a free cytochrome or as one of multiple cytochrome-type or cytochrome superfamily domains. In rare or isolated cases, C1 homologs co-occur in ORFs with membrane or structural protein domains (Table A3). The ORF containing the C1 homolog was annotated as a NOR in several members of the Nitrospirae and one Geobacteraceae genome (Table A3); domain analysis of these genes yielded limited additional data, but representative sequences showed detectable sequence similarity to *Pseudomonas norC* genes.

The occurrence of C1 domain homologs within predicted nitrite reductase genes is restricted to the Chloroflexi. The majority of these C1-containing *nir* genes have the cytochrome-type NirS domain; however, a small number of Chloroflexi MAGs contain an ORF pairing the C1 cytochrome with the copper-type NirK domain instead. This NirK ORF also included an N-terminal cupredoxin/plastocyanin domain. As this fusion is only apparent within a small number of MAGs, which are identical across the length of the analyzed ORF, this may represent an assembly artifact. However, several of the *nir* genes that contained a C1 homolog and a cytochrome-type NirS (not copper-type NirK) also contained cupredoxins or other copper-containing domains (Figure A6).

The distinct phylogeny and taxonomic distribution of C1, as compared with C2 and NirS domains, strongly suggest that the C1-C2-NirS domain structure observed in Chloroflexi is the result of a fusion of the C1 domain with a horizontally-acquired *nir* gene containing the C2 and NirS domains. Topology and extant taxon sampling of these gene trees does not allow us to reliably infer the donor lineage of this transfer. However, the C2-NirS architecture—or similar arrangements of functional domains—is widespread among members of the Alpha-, Beta-, and Gammaproteobacteria; additionally, gene trees for C2 and NirS place the Chloroflexi that also contain the C1 domain within (Figure 4) or as sister to (Figures A4 and A5) Proteobacterial groups, inconsistent with species tree placements for these phyla. These data suggest the Proteobacteria as a possible donor group for the C2-NirS domains. Additionally, it appears that Chloroflexi may have been the source for an independent transfer of the free C1 domain into Nitrospirae and Nitrospinae.

3.2 | C1-C2-NirS domain architecture is unique to Chloroflexi

Though putative homologs exist independently for the constituent C1 and C2-NirS regions, respectively, these hits reflect different cytochrome or cytochrome-type nitrite reductases (largely in Proteobacteria, Nitrospirae, and Nitrospinae). The full C1-C2-NirS architecture appears unique to Chloroflexi and is not observed in other groups. Querying NCBI's nonredundant environmental database

FIGURE 4 Phylogenetic trees for C2 and NirS domains. Phylogenetic analysis of C2 domain homologs (above) places the Chloroflexi within a diverse clade including Epsilonproteobacteria, Aquificae, Bacteroidetes, and Planctomycetes; this clade is sister to a broad radiation of Alpha-, Beta-, and Gammaproteobacteria. Analysis of NirS domain homologs (below) places the Chloroflexi within the clade dominated by Alpha-, Beta-, and Gammaproteobacteria, which also contains members of the Bacteroidetes and Aquificales. The overall taxonomic representation for the domains is similar. Support values for selected bipartitions are labeled (aLRT/bb). Support for other nodes is indicated with the following color scheme: Strong support with both values ≥90 (black); weak support with both values ≤50 (white); intermediate support with one or both values between 50 and 90 (gray); conflicting support, with one value ≤50 and the other ≥90 (gray)

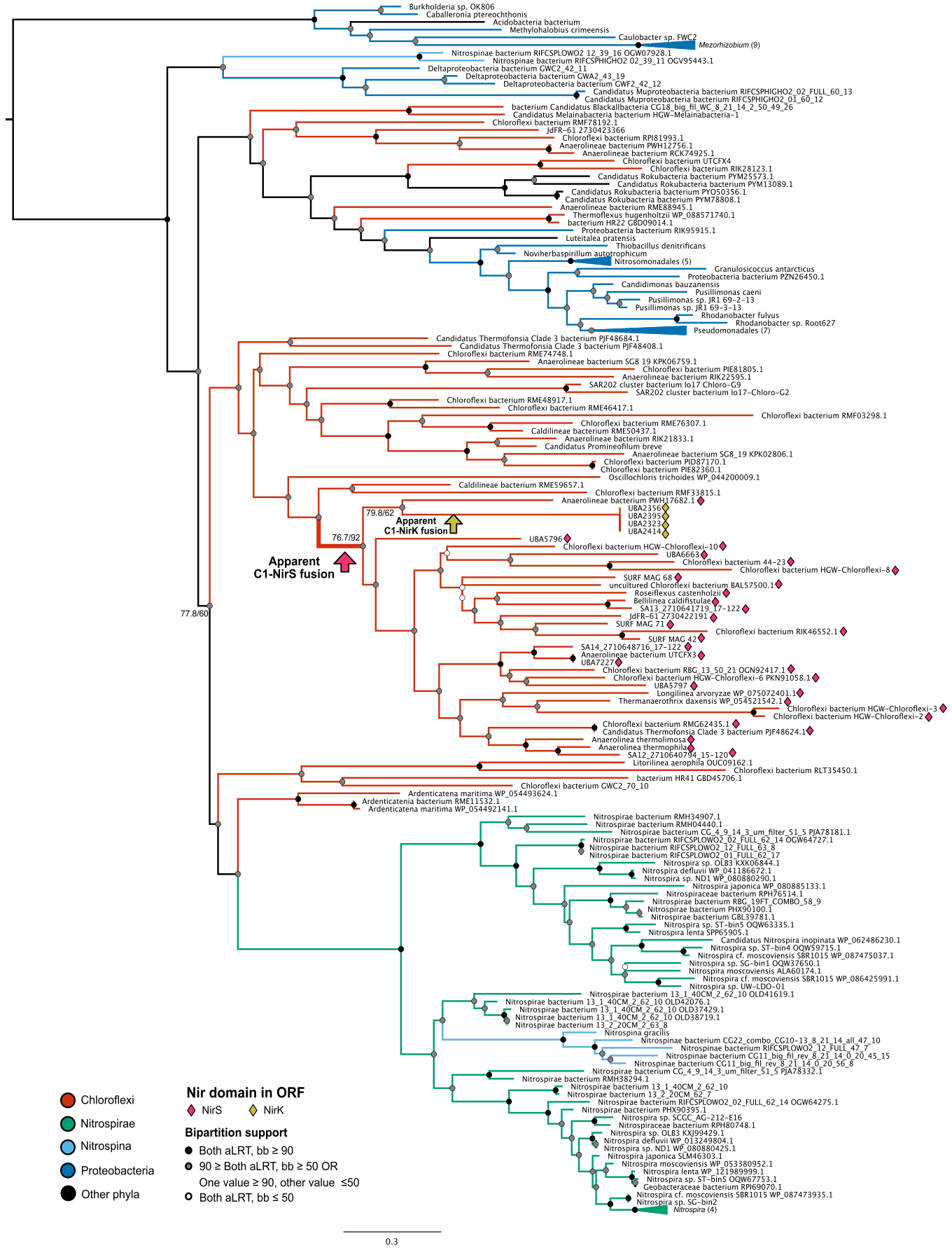

FIGURE 5 (See caption on next page)

(env-nr) with the full ORF from SURF MAG 42 did not identify additional examples of the full gene construct. While several hits were identified that reflected putative homology to the joint C2-NirS domains, none of these included the C1 domain as well. An independent search of the env-nr database using the C1 domain as a query returned few overall hits. While some of these putative C1 homologs were identified in ORFs containing additional cytochrome-type enzyme superfamily domains or subunits, none co-occurred with NirS or NirK domains. These data suggest that there is little to no missing diversity of the Chloroflexi-type chimeric nitrite reductase in existing metagenomes.

Attempts to visualize the full enzyme structure using homology modeling (Bienert et al., 2017; A. Waterhouse et al., 2018) were unsuccessful; structural models were only able to predict a close match for the conserved C2-NirS region of the putative gene. Efforts to independently model the C1 structure could not recover predicted QMEAN scores above −4.50 (Benkert et al., 2011). The poor scores may reflect the relatively short length of the cytochrome coding region. However, the Chloroflexi *nirS* gene sequence does retain several conserved residues present in the crystal structure of *P. aeruginosa* NirS. In *P. aeruginosa* NirS, His51, and Met88 coordinate heme *c*; His182 coordinates heme d1; and His327 and His369 are believed to stabilize the active site nitrite anion (Maia & Moura, 2014; Rinaldo et al., 2011). Corresponding residues are conserved within the C2 (His65, Met125) and NirS alignments (His46, His239, His300) for the Chloroflexi NirS ORF; interestingly, the residue corresponding to His327 (His239) is not universally conserved, though it is conserved among Chloroflexi with the novel NirS architecture.

3.3 | Expansion of eNOR diversity

Notably, the majority of genomes with the unique C1-C2-NirS structure do not appear to contain a NOR gene (*nor*). Though the absence of the *nor* gene in genomes with *nirS* is not unprecedented, previous genomic surveys suggest it is relatively uncommon, and the toxicity of the product of Nir (NO) makes this absence counterintuitive (Graf et al., 2014; Hendriks et al., 2000). However, analysis of the SURF MAG 42 metagenome—the originally assembled genome in which the novel *nirS* ORF was observed—did reveal the presence of an unusual *nor* homolog. Previous studies have identified the established cNOR and qNOR family enzymes (which contain cytochrome c or quinols as electron donors, respectively) in Chloroflexi, as well as a broad distribution of Proteobacteria (Hemp & Gennis, 2008; Hendriks et al., 2000; Zumft, 2005). However, the predicted NOR in SURF MAG 42 included an active site glutamine substitution characteristic of eNOR (Hemp & Gennis, 2008; Hemp et al., 2015; Table A4). SURF MAG 42 contains both proposed subunits (Hemp & Gennis, 2008) of eNOR; the diagnostic subfamily substitution is within the heme-copper cytochrome-containing subunit I, and the cupredoxin-containing subunit II is immediately upstream in the MAG (Figure A7). eNOR has been previously described in Archaea (Hemp & Gennis, 2008) and at least one isolated Anaerolineales bacterium (Hemp et al., 2015).

Phylogenetic analysis indicates the presence of *eNOR* in an expanded diversity of genomes (Figure 6). Previous studies have described eNOR in *Natronomonas*; these data indicate a cluster of *eNOR* genes throughout other Halobacteria as well. Additional putative *eNOR* genes appear in multiple members of Anaerolineales, as well as other Chloroflexi, and in many members of the Alpha-, Beta-, Gamma-, and Deltaproteobacteria. Many of these putative *eNOR* subunit homologs appear to have been misannotated or mislabeled as cytochrome *c* oxidase genes, likely because of the structural similarity of the heme–copper cytochrome region (Hemp & Gennis, 2008; Marchler-Bauer et al., 2015).

4 | DISCUSSION

The phylogenetic analyses of *nirS* and *eNOR* ORFs in Chloroflexi suggest that subsurface ecosystems may harbor an under-described diversity of denitrification enzymes, which may reflect adaptations to the unique challenges of nutrient cycling within these environments. More broadly, a deeper understanding of the ecological extent of microbial denitrification has important implications for basic and applied microbial ecology. The reduction of fixed nitrogen species plays a crucial role in global nitrogen cycling and is also an essential component of smaller-scale systems, such as those associated with agricultural or waste treatment (Butterbach-Bahl & Dannenmann, 2011; H. Lu et al., 2014). The discovery and characterization of novel variants of genes such as *nirS* and *eNOR* may therefore pave the way for future biotechnological applications.

Although the C2 and NirS domains do not have identical evolutionary histories or distributions, the taxonomic representation of these groups is very similar, and the presence of the paired C2-NirS domains in cytochrome-type nitrite reductases appears broadly throughout the Proteobacteria. In contrast, the taxonomic distribution and phylogeny of the C1 domain tree are strikingly different than

FIGURE 5 Phylogenetic tree for C1 domain. A phylogenetic tree for the C1 domain—with no genus-level filter and inclusion of more distant hits (see Methods)—indicates a limited taxonomic distribution of the domain. The largest group of sequences in Chloroflexi places sister to domains found in Nitrospirae, Nitrospinae, and Deltaproteobacteria. Within this clade, the branch along which C1 is inferred to have fused into nitrite reductase genes in Chloroflexi is labeled. C1 homologs that co-occur in ORFs with nitrite reductase are indicated with magenta diamonds (NirS) or yellow diamonds (NirK). Support values for selected bipartitions are labeled (aLRT/bb). Support for other nodes is indicated with the following color scheme: Strong support with both values ≥90 (black); weak support with both values ≤50 (white); intermediate support with one or both values between 50 and 90 (gray); conflicting support, with one value ≤50 and the other ≥90 (gray). ORF, open reading frame

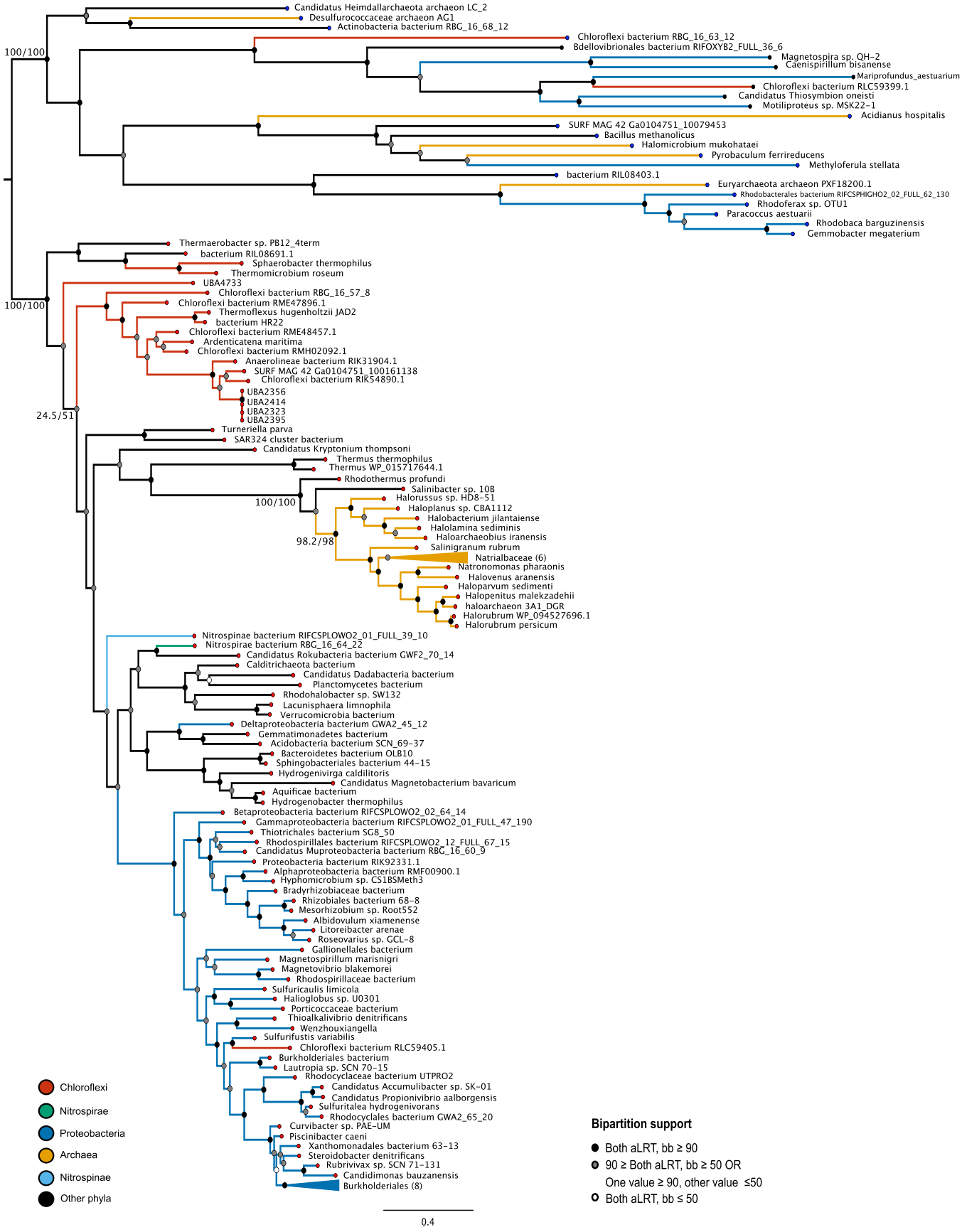

FIGURE 6 (See caption on next page)

that of the other domains in the nitrite reductase ORF. Combined with the apparent absence of a full C1-C2-NirS ORF in any taxonomic group other than Chloroflexi, these data suggest that the C1 cytochrome was likely incorporated into *nirS* in a gene fusion event within Chloroflexi, following HGT. As there is no evidence of the C2-NirS ORF in Chloroflexi without the fused C1 domain present, the fusion probably occurred very soon after the acquisition of the C2-NirS region and may be necessary for the function of the gene in Chloroflexi.

In *P. aeruginosa*, cytochrome c551—encoded by *nirM*—is the electron donor for the adjacent cytochrome *cd1 nirS* (Philippot, 2002; Zumft, 1997). Homology searches do not identify any regions within SURF MAG 42 with significant similarity to *Pseudomonas nirM*, but C1 is identified as a putative member of the cytochrome c551/552 family. It is, therefore, possible that C1, though divergent from Proteobacterial *nirM*, serves a similar redox role for the cytochrome *cd1* now within the same ORF.

Interestingly, putative homologs of C1 cytochrome domains were found in some Chloroflexi genomes in ORFs containing *nirK*, not *nirS* (Figures 5 and A6). Though NirS and NirK are functionally equivalent, the two enzymes do not show a shared evolutionary origin and are often—though not always—mutually exclusive among known denitrifier genomes (Graf et al., 2014; Jones et al., 2008). Unlike the cytochrome-containing NirS, NirK is a copper-type enzyme. The co-occurrence of cytochrome *c* domains in ORFs with the copper-type *nirK* has been identified in rare instances in Proteobacteria, and noted as surprising, given the cupredoxin-like fold of the NirK enzyme (Bertini et al., 2006). Similarly surprising is the inverse relationship revealed in the C1 domain tree: Several Chloroflexi ORFs contain a cupredoxin or similar copper-containing domain N-terminal to the C1-C2-NirS architecture (Figure A6, Table A3). The co-occurrence of C1 with both cytochrome- and copper-dependent Nir domains suggests a general evolutionary trend within Chloroflexi to incorporate this cytochrome into denitrification ORFs. This distribution pattern raises the possibility that the C1-type cytochrome may serve an important but generalized role in nitrite reduction—regardless of the evolutionary history or genetic profile of the nitrite reduction domain itself.

The apparent absence of a *nor* homolog in the majority of genomes with the C1-*nirS* fusion is unexpected. Beyond providing downstream redox capacity, NOR provides an efficient means of reducing and detoxifying NO, the highly cytotoxic product of NirS. It is not unprecedented for bacterial genomes to harbor a *nir* gene without a *nor* gene, particularly for organisms with *nirK* (Graf et al., 2014; Heylen et al., 2007). This *nir–nor* mismatch is much rarer for putative denitrifiers with *nirS*, representing fewer than 4% of genomes in a recent survey—but a small number of surveyed bacteria do, interestingly, appear to harbor *nirS* without also harboring *cNOR* or *qNOR* (Graf et al., 2014; Heylen et al., 2007). To our knowledge, however, *eNOR* has not been included in such analyses of the genomic correlation between nitrite reductases and NORs. The phylogenetic evidence for diverse *eNOR* homologs suggests likely undocumented or underexplored diversity for divergent NORs. The diversity and function of cNOR and qNOR are fairly well-established. However, divergent enzymes such as eNOR and sNOR are less extensively documented and may not be accurately distinguished from broader oxygen reductase superfamily members in genomic or metagenomic analyses.

Cytochrome *c* proteins function as electron transfer proteins in anaerobic respiration and are often fused to redox enzymes to allow electron passage (Bertini et al., 2006). It is not surprising, therefore, to find cytochrome *c*-containing subunits in frame with nitrite reductase. NirS itself is cytochrome-dependent (Bertini et al., 2006). However, the unusual addition of the upstream cytochrome domain (C1) may reflect additional redox requirements or capacity. It is also possible that the inclusion of this construct could be linked to the conspicuous absence of NOR enzymes in several MAGs containing a NirS ORF with the C1 fusion. NO reduction can be cytochrome-dependent; the well-studied cNORs contain a membrane-anchored cytochrome *c* (Hemp & Gennis, 2008). Further, the C1 domain tree recovers ORFs in the Nitrospirae that contain C1 homologs and are annotated as NORs, with detectable similarity to Proteobacteria NOR subunits. It is therefore possible that the inclusion of a C1 domain in *nir* genes within genomes lacking *eNOR* reflects some generalized NOR-like role in detoxification of the cytotoxic product of NirS. Additionally, while the presence of NirS suggests an active denitrification pathway, and the NirS domain tree reflects the homology between this domain and NirS from known denitrifying groups, the possibility remains that this group of Chloroflexi do not perform denitrification, and instead use this gene product for a different metabolic function, potentially enabled or constrained by the C1 domain. The genetic diversity observed within C1-C2-NirS gene neighborhoods—varying both from the genetic makeup of a canonical denitrification operon, and between different Chloroflexi MAGs—may reflect such functional flexibility. Shared or convergent functions could also be recovered among these diverse neighborhoods. The analyzed gene neighborhoods suggest some conserved functionality between different genomes from varying environmental sources and

FIGURE 6 *eNOR* gene tree. A phylogenetic tree of homologs to the nitric oxide reductase from SURF MAG 42 reveals an expanded diversity of putative *eNOR* subunit I homologs in not only Archaea and Chloroflexi, but also Proteobacteria and other diverse phyla. Putative *eNOR* sequences (red tips) have the characteristic Gln-323 in the alignment; outgroup sequences (blue tips) have Tyr-323 (oxygen reductase superfamily) or other substitutions. Support values for selected bipartitions are labeled (aLRT/bb). Support for other nodes is indicated with the following color scheme: Strong support with both values ≥90 (black); weak support with both values ≤50 (white); intermediate support with one or both values between 50 and 90 (gray); conflicting support, with one value ≤50 and the other ≥90 (gray). MAG, metagenome-assembled genome; SURF, Sanford Underground Research Facility

samples; for example, the presence of heme–copper oxidase subunits, molybdenum cofactor enzymes, and NADB Rossman superfamily proteins (Tables A1 and A2). However, without expanded homology analyses and experimental validation, it is impossible to infer whether apparent similarities or differences reflect biologically-meaningful patterns of inheritance or function, or are simply artifactual.

A divergent or generalized role is also possible for the eNOR homologs. Models indicate that eNOR (unlike related NORs cNOR, qNOR, sNOR, and gNOR) has a proton channel, and therefore the capacity for proton pumping (Hemp & Gennis, 2008); therefore, this gene product may serve a key electrogenic role, whether reducing NO or alternative substrates. Experimental validation would be necessary to determine if the novel Chloroflexi-associated NirS performs differently than canonical NirS in vivo, and if NirS and eNOR perform targeted denitrification or nonspecific detoxification or proton pumping. This study, therefore, suggests a promising direction for future investigations.

The divergent denitrification enzymes described above may or may not reflect different metabolic strategies in situ. But the identification of both a novel *nirS* ORF and an expanded diversity of eNOR enzymes suggests that the existing understanding of denitrification may underestimate the genetic diversity and ecological distribution of constituent enzymes. This may be especially true in deep subsurface biomes, such as those from which several Chloroflexi analyzed in this study were isolated. These systems have garnered increasing attention in recent years; extensive evidence supports the existence of dynamic, diverse microbial subsurface ecosystems with the metabolic potential to influence global biogeochemical cycles (Hug et al., 2013; Magnabosco et al., 2018; Momper & Jungbluth, 2017; Osburn et al., 2014, 2019). Chloroflexi are frequently cited as well-represented members of deep sediment and aquifer systems, where they play key roles in carbon cycling dynamics (Hug et al., 2013; Kadnikov et al., 2020; Momper & Jungbluth, 2017; Momper & Kiel Reese, 2017). But Chloroflexi are known to also harbor diverse nitrogen metabolisms (Denef et al., 2016; Hemp et al., 2015; Spieck et al., 2020), and previous studies have linked subsurface Chloroflexi to denitrification pathway genes such as nitrous oxide reductase (*nos*) (Hug et al., 2016; Momper & Jungbluth, 2017; Sanford et al., 2012). The role of Chloroflexi in subsurface nitrogen cycling—as well as the scope of subsurface microbial nitrogen dynamics at large—requires further investigation.

ACKNOWLEDGMENTS

The authors thank Dr. Ranjani Murali for advice on domain and residue identification and analysis. This study was supported by a National Defense Science and Engineering Graduate Fellowship to Sarah L. Schwartz, and Simons Collaboration on Origins of Life award #339603 to Gregory P. Fournier.

CONFLICT OF INTEREST

None declared.

ETHICS STATEMENT

None required.

AUTHOR CONTRIBUTIONS

Sarah L. Schwartz: Conceptualization (supporting), Data curation (lead), Formal analysis (lead), Funding acquisition (equal), Investigation (lead), Methodology (lead), Project administration (lead), Validation (equal), Visualization (lead), Writing – original draft (lead), Writing – review & editing-Lead. **Lily M. Momper**: Conceptualization (lead); Data curation (supporting); Investigation (supporting); Methodology (supporting); Writing – original draft (supporting). **L. Thiberio Rangel**: Data curation (supporting), Investigation (supporting), Methodology (equal), Writing – review & editing (supporting). **Cara Magnabosco**: Data curation (supporting), Investigation (supporting), Methodology (supporting). **Jan P. Amend**: Conceptualization (supporting), Data curation (supporting), Project administration (supporting), Resources (supporting), Writing – review & editing (supporting). **Gregory P. Fournier**: Conceptualization (supporting), Formal analysis (supporting), Funding acquisition (equal), Investigation (supporting), Methodology (supporting), Project administration (lead), Resources (lead), Supervision (lead), Writing – review & editing (lead).

DATA AVAILABILITY STATEMENT

The data that support the findings of this study are openly available in figshare at https://doi.org/10.6084/m9.figshare.14515554.v2. Scripts used to automate analyses are archived in Zenodo at https://doi.org/10.5281/zenodo.5745924.

ORCID

Sarah L. Schwartz http://orcid.org/0000-0003-2239-3565
Jan P. Amend https://orcid.org/0000-0003-4953-7776

REFERENCES

Agarwala, R., Barrett, T., Beck, J., Benson, D. A., Bollin, C., Bolton, E., Bourexis, D., Brister, J. R., Bryant, S. H., Canese, K., Cavanaugh, M., Charowhas, C., Clark, K., Dondoshansky, I., Feolo, M., Fitzpatrick, L., Funk, K., Geer, L. Y., Gorelenkov, V., … Zbicz, K. (2018). Database resources of the National Center for Biotechnology Information. *Nucleic Acids Research*, *46*, D8–D13. https://doi.org/10.1093/nar/gkx1095

Al-Attar, S., & de Vries, S. (2015). An electrogenic nitric oxide reductase. *FEBS Letters*, *589*(16), 2050–2057. http://doi.org/10.1016/j.febslet.2015.06.033

Alneberg, J., Bjarnason, B. S., de Bruijn, I., Schirmer, M., Quick, J., Ijaz, U. Z., Lahti, L., Loman, N. J., Andersson, A. F., & Quince, C. (2014). Binning metagenomic contigs by coverage and composition. *Nature Methods*, *11*, 1144–1146. https://doi.org/10.1038/nmeth.3103

Benkert, P., Biasini, M., & Schwede, T. (2011). Toward the estimation of the absolute quality of individual protein structure models. *Bioinformatics*, *27*(3), 343–350. http://doi.org/10.1093/bioinformatics/btq662

Berman, H. M., Westbrook, J., Feng, Z., Gilliland, G., Bhat, T. N., Weissig, H., Shindyalov, I. N., & Bourne, P. E. (2000). The Protein Data Bank. *Nucleic Acids Research*, *28*, 235–242. https://doi.org/10.1093/nar/28.1.235

Bertini, I., Cavallaro, G., & Rosato, A. (2006). Cytochrome c: Occurrence and functions. *Chemical Reviews*, *106*, 90–115. https://doi.org/10.1021/cr050241v

Bienert, S., Waterhouse, A., de Beer, T. A., Tauriello, G., Studer, G., Bordoli, L., & Schwede, T. (2017). The SWISS-MODEL Repository-new features and functionality. *Nucleic Acids Research*, *45*, D313–D319. https://doi.org/10.1093/nar/gkw1132

Blomberg, M. R. A., & Ädelroth, P. (2018). Mechanisms for enzymatic reduction of nitric oxide to nitrous oxide—a comparison between nitric oxide reductase and cytochrome c oxidase. *Biochimica et Biophysica Acta—Bioenergetics*, *1859*(11), 1223–1234. https://doi.org/10.1016/j.bbabio.2018.09.368

Braker, G., Zhou, J., Wu, L., Devol, A. H., & Tiedje, J. M. (2000). Nitrite reductase genes (nirK and nirS) as functional markers to investigate diversity of denitrifying bacteria in pacific northwest marine sediment communities. *Applied and Environmental Microbiology*, *66*(5), 2096–2104. https://doi.org/10.1128/AEM.66.5.2096-2104.2000

Butterbach-Bahl, K., & Dannenmann, M. (2011). Denitrification and associated soil N_2O emissions due to agricultural activities in a changing climate. *Current Opinion in Environmental Sustainability*, *3*(5), 389–395. https://doi.org/10.1016/j.cosust.2011.08.004

Camacho, C., Coulouris, G., Avagyan, V., Ma, N., Papadopoulos, J., Bealer, K., & Madden, T. L. (2009). BLAST+: Architecture and applications. *BMC Bioinformatics*, *10*, 403. https://doi.org/10.1186/1471-2105-10-421

Campbell, J. H., O'Donoghue, P., Campbell, A. G., Schwientek, P., Sczyrba, A., Woyke, T., Söll, D., & Podar, M. (2013). UGA is an additional glycine codon in uncultured SR1 bacteria from the human microbiota. *Proceedings of the National Academy of Sciences of the United States of America*, *110*, 5540–5545. https://doi.org/10.1073/pnas.1303090110

Canfield, D. E., Glazer, A. N., & Falkowski, P. G. (2010). The evolution and future of earth's nitrogen cycle. *Science*, *330*(6001), 192–196. https://doi.org/10.1126/science.1186120

Creevey, C. J., Doerks, T., Fitzpatrick, D. A., Raes, J., & Bork, P. (2011). Universally distributed single-copy genes indicate a constant rate of horizontal transfer. *PLoS One*, *6*(8), e22099. https://doi.org/10.1371/journal.pone.0022099

Decleyre, H., Heylen, K., Tytgat, B., & Willems, A. (2016). Erratum to: Highly diverse nirK genes comprise two major clades that harbour ammonium-producing denitrifiers. *BMC Genomics*, *17*(1), 12864. https://doi.org/10.1186/s12864-016-2812-1

Denef, V. J., Mueller, R. S., Chiang, E., Liebig, J. R., & Vanderploeg, H. A. (2016). Chloroflexi CL500-11 populations that predominate deep-lake hypolimnion bacterioplankton rely on nitrogen-rich dissolved organic matter metabolism and C1 compound oxidation. *Applied and Environmental Microbiology*, *82*(5), 1423–1432. https://doi.org/10.1128/AEM.03014-15

Dupont, C. L., Rusch, D. B., Yooseph, S., Lombardo, M. J., Richter, R. A., Valas, R., Novotny, M., Yee-Greenbaum, J., Selengut, J. D., Haft, D. H., Halpern, A. L., Lasken, R. S., Nealson, K., Friedman, R., & Venter, J. C. (2012). Genomic insights to SAR86, an abundant and uncultivated marine bacterial lineage. *ISME Journal*, *6*(6), 1186–1199. https://doi.org/10.1038/ismej.2011.189

Gardner, A. M., Helmick, R. A., & Gardner, P. R. (2002). Flavorubredoxin, an inducible catalyst for nitric oxide reduction and detoxification in *Escherichia coli*. *Journal of Biological Chemistry*, *277*(10), 8172–8177. https://doi.org/10.1074/jbc.M110471200

Graf, D. R. H., Jones, C. M., & Hallin, S. (2014). Intergenomic comparisons highlight modularity of the denitrification pathway and underpin the importance of community structure for N_2O emissions. *PLoS One*, *9*(12), 1–20. https://doi.org/10.1371/journal.pone.0114118

Harrison, K. J., Crécy-Lagard, De, V., & Zallot, R. (2018). Gene graphics: A genomic neighborhood data visualization web application. *Bioinformatics*, *34*(8), 1406–1408. https://doi.org/10.1093/bioinformatics/btx793

Heard, A. W., Warr, O., Borgonie, G., Linage-Alvarez, B., Kuloyo, O., Magnabosco, C., Lau, M., Erasmus, M., Cason, E. D., van Heerden, E., Kieft, T. L., Mabry, J., Onstott, T. C., Sherwood Lollar, B., & Ballentine, C. J. (2017). Origins and ages of fracture fluids in the South African Crust [Abstract]. *American Geophysical Union, Fall Meeting*, *H11A–H11153*.

Hemp, J., Ward, L. M., Pace, L. A., & Fischer, W. W. (2015). Draft genome sequence of *Ardenticatena maritima* 110S, a thermophilic nitrate- and iron-reducing member of the Chloroflexi Class Ardenticatenia. *Genome Announcements*, *3*(6), 2920. https://doi.org/10.1128/genomeA.01347-15

Hemp, J., & Gennis, R. B. (2008). Diversity of the heme-copper superfamily in archaea: Insights from genomics and structural modeling. *Results and Problems in Cell Differentiation*, *45*, 1–31. https://doi.org/10.1007/400_2007_046

Hendriks, J., Oubrie, A., Castresana, J., Urbani, A., Gemeinhardt, S., & Saraste, M. (2000). Nitric oxide reductases in bacteria. *Biochimica et Biophysica Acta—Bioenergetics*, *1459*(2–3), 266–273. https://doi.org/10.1016/S0005-2728(00)00161-4

Heylen, K., Vanparys, B., Gevers, D., Wittebolle, L., Boon, N., & De Vos, P. (2007). Nitric oxide reductase (norB) gene sequence analysis reveals discrepancies with nitrite reductase (nir) gene phylogeny in cultivated denitrifiers. *Environmental Microbiology*, *9*(4), 1072–1077. https://doi.org/10.1111/j.1462-2920.2006.01194.x

Hoang, D. T., Chernomor, O., von Haeseler, A., Minh, B. Q., & Vinh, L. S. (2018). UFBoot2: Improving the ultrafast bootstrap approximation. *Molecular Biology and Evolution*, *35*, 518–522. https://doi.org/10.1093/molbev/msx281

Hug, L. A., Castelle, C. J., Wrighton, K. C., Thomas, B. C., Sharon, I., Frischkorn, K. R., Williams, K. H., Tringe, S. G., & Banfield, J. F. (2013). Community genomic analyses constrain the distribution of metabolic traits across the Chloroflexi phylum and indicate roles in sediment carbon cycling. *Microbiome*, *1*(1), 1–17. https://doi.org/10.1186/2049-2618-1-22

Hug, L. A., Thomas, B. C., Sharon, I., Brown, C. T., Sharma, R., Hettich, R. L., Wilkins, M. J., Williams, K. H., Singh, A., & Banfield, J. F. (2016). Critical biogeochemical functions in the subsurface are associated with bacteria from new phyla and little studied lineages. *Environmental Microbiology*, *18*(1), 159–173. https://doi.org/10.1111/1462-2920.12930

Huntemann, M., Ivanova, N. N., Mavromatis, K., Tripp, H. J., Paez-Espino, D., Palaniappan, K., Szeto, E., Pillay, M., Chen, I. M., Pati, A., Nielsen, T., Markowitz, V. M., & Kyrpides, N. C. (2015). The standard operating procedure of the DOE-JGI Microbial Genome Annotation Pipeline (MGAP v.4). *Standards in Genomic Sciences*, *11*, 27. https://doi.org/10.1186/s40793-015-0077-y

Jones, C. M., Stres, B., Rosenquist, M., & Hallin, S. (2008). Phylogenetic analysis of nitrite, nitric oxide, and nitrous oxide respiratory enzymes reveal a complex evolutionary history for denitrification. *Molecular Biology and Evolution*, *25*(9), 1955–1966. https://doi.org/10.1093/molbev/msn146

Jungbluth, S. P., Amend, J. P., & Rappé, M. S. (2017). Corrigendum: Metagenome sequencing and 98 microbial genomes from Juan de Fuca Ridge flank subsurface fluids. *Scientific Data*, *4*, 170080. https://doi.org/10.1038/sdata.2017.80

Kadnikov, V. V., Mardanov, A. V., Beletsky, A. V., Karnachuk, O. V., & Ravin, N. V. (2020). Microbial life in the deep subsurface aquifer illuminated by metagenomics. *Frontiers in Microbiology*, *11*, 1–15. https://doi.org/10.3389/fmicb.2020.572252

Kalyaanamoorthy, S., Minh, B. Q., Wong, T., von Haeseler, A., & Jermiin, L. S. (2017). ModelFinder: Fast model selection for accurate phylogenetic estimates. *Nature Methods*, *14*, 587–589. https://doi.org/10.1038/nmeth.4285

Kawasaki, S., Arai, H., Kodama, T., & Igarashi, Y. (1997). Gene cluster for dissimilatory nitrite reductase (nir) from *Pseudomonas aeruginosa*: Sequencing and identification of a locus for heme d1 biosynthesis. *Journal of Bacteriology*, *179*(1), 235–242. https://doi.org/10.1128/jb.179.1.235-242.1997

Kluyver, T., Ragan-Kelley, B., Pérez, F., Granger, B., Bussonnier, M., Frederic, J., Kelley, K., Hamrick, J., Grout, J., Corlay, S., Ivanov, P.,

Avila, D., Abdalla, S., Willing, C., & Jupyter Development Team (2016). *Jupyter Notebooks—a publishing format for reproducible computational workflows* (Vol. 2016, pp. 87–90). ELPUB. https://doi.org/10.3233/978-1-61499-649-1-87

Lau, M. C., Cameron, C., Magnabosco, C., Brown, C. T., Schilkey, F., Grim, S., Hendrickson, S., Pullin, M., Sherwood Lollar, B., van Heerden, E., Kieft, T. L., & Onstott, T. C. (2014). of functional genes shared among seven terrestrial subsurface metagenomes reveal N-cycling and microbial evolutionary relationships. *Frontiers in Microbiology*, *5*, 1–17. https://doi.org/10.3389/fmicb.2014.00531

Lau, M. C., Kieft, T. L., Kuloyo, O., Linage-Alvarez, B., van Heerden, E., Lindsay, M. R., Magnabosco, C., Wang, W., Wiggins, J. B., Guo, L., Perlman, D. H., Kyin, S., Shwe, H. H., Harris, R. L., Oh, Y., Yi, M. J., Purtschert, R., Slater, G. F., Ono, S., … Onstott, T. C. (2016). An oligotrophic deep-subsurface community dependent on syntrophy is dominated by sulfur-driven autotrophic denitrifiers. *Proceedings of the National Academy of Sciences of United States of America*, *113*(49), E7927–E7936. https://doi.org/10.1073/pnas.1612244113

Lu, H., Chandran, K., & Stensel, D. (2014). *Microbial ecology of denitrification in biological wastewater treatment*, *Water Research* (Vol. 64, pp. 237–254). Elsevier Ltd. https://doi.org/10.1016/j.watres.2014.06.042

Lu, S., Wang, J., Chitsaz, F., Derbyshire, M. K., Geer, R. C., Gonzales, N. R., Gwadz, M., Hurwitz, D. I., Marchler, G. H., Song, J. S., Thanki, N., Yamashita, R. A., Yang, M., Zhang, D., Zheng, C., Lanczycki, C. J., & Marchler-Bauer, A. (2020). CDD/SPARCLE: The conserved domain database in 2020. *Nucleic Acids Research*, *48*, D265–D268. https://doi.org/10.1093/nar/gkz991

Magnabosco, C., Ryan, K., Lau, M. C. Y., Kuloyo, O., Lollar, B. S., Kieft, T. L., van Heerden, E., & Onstott, T. C. (2016). A metagenomic window into carbon metabolism at 3 km depth in Precambrian continental crust. *ISME Journal*, *10*(3), 730–741. https://doi.org/10.1038/ismej.2015.150

Magnabosco, C., Lin, L. H., Dong, H., Bomberg, M., Ghiorse, W., Stan-Lotter, H., Pedersen, K., Kieft, T. L., van Heerden, E., & Onstott, T. C. (2018). The biomass and biodiversity of the continental subsurface. *Nature Geoscience*, *11*(10), 707–717. https://doi.org/10.1038/s41561-018-0221-6

Maia, L. B., & Moura, J. J. G. (2014). How biology handles nitrite. *Chemical Reviews*, *114*(10), 5273–5357. https://doi.org/10.1021/cr400518y

Marchler-Bauer, A., Derbyshire, M. K., Gonzales, N. R., Lu, S., Chitsaz, F., Geer, L. Y., Geer, R. C., He, J., Gwadz, M., Hurwitz, D. I., Lanczycki, C. J., Lu, F., Marchler, G. H., Song, J. S., Thanki, N., Wang, Z., Yamashita, R. A., Zhang, D., Zheng, C., & Bryant, S. H. (2015). CDD: NCBI's conserved domain database. *Nucleic Acids Research*, *43*, D222–D226. https://doi.org/10.1093/nar/gku1221

Markowitz, V. M., Ivanova, N. N., Szeto, E., Palaniappan, K., Chu, K., Dalevi, D., Chen, I. M., Grechkin, Y., Dubchak, I., Anderson, I., Lykidis, A., Mavromatis, K., Hugenholtz, P., & Kyrpides, N. C. (2008). IMG/M: A data management and analysis system for metagenomes. *Nucleic Acids Research*, *36*, D534–D538. https://doi.org/10.1093/nar/gkm869

Matsuura, N., Tourlousse, D. M., Ohashi, A., Hugenholtz, P., & Sekiguchi, Y. (2015). Draft Genome Sequences of *Anaerolinea thermolimosa* IMO-1, *Bellilinea caldifistulae* GOMI-1, Leptolinea tardivitalis YMTK-2, *Levilinea saccharolytica* KIBI-1, *Longilinea arvoryzae* KOME-1, previously described as members of the Class Anaerolineae (Chloroflexi). *Genome Announcements*, *3*(5), e00975-15. https://doi.org/10.1128/genomeA.00975-15

Minh, B. Q., Nguyen, M. A. T., & Von Haeseler, A. (2013). Ultrafast approximation for phylogenetic bootstrap. *Molecular Biology and Evolution*, *30*, 1188–1195. https://doi.org/10.1093/molbev/mst024

Mitchell, A. L., Attwood, T. K., Babbitt, P. C., Blum, M., Bork, P., Bridge, A., Brown, S. D., Chang, H. Y., El-Gebali, S., Fraser, M. I., Gough, J., Haft, D. R., Huang, H., Letunic, I., Lopez, R., Luciani, A., Madeira, F., Marchler-Bauer, A., Mi, H., … Finn, R. D. (2019). InterPro in 2019: Improving coverage, classification and access to protein sequence annotations. *Nucleic Acids Research*, *47*, D351–D360. https://doi.org/10.1093/nar/gky1100

Momper, L., Jungbluth, S. P., Lee, M. D., & Amend, J. P. (2017). Energy and carbon metabolisms in a deep terrestrial subsurface fluid microbial community. *ISME Journal*, *11*(10), 2319–2333. https://doi.org/10.1038/ismej.2017.94

Momper, L., Kiel Reese, B., Zinke, L., Wanger, G., Osburn, M. R., Moser, D., & Amend, J. P. (2017). Major phylum-level differences between porefluid and host rock bacterial communities in the terrestrial deep subsurface. *Environmental Microbiology Reports*, *9*(5), 501–511. https://doi.org/10.1111/1758-2229.12563

Murali, R., Hemp, J., Orphan, V., & Bisk, Y. (2019). FIND: Identifyingfunctionally and structurally important features in protein sequences with deep neural networks. *bioRxiv*. https://doi.org/10.1101/592808

Nakamura, T., Yamada, K. D., Tomii, K., & Katoh, K. (2018). Parallelization of MAFFT for large-scale multiple sequence alignments'. *Bioinformatics*, *34*, 2490–2492. https://doi.org/10.1093/bioinformatics/bty121

Nguyen, L. T., Schmidt, H. A., von Haeseler, A., & Minh, B. Q. (2015). IQ-TREE: A fast and effective stochastic algorithm for estimating maximum-likelihood phylogenies. *Molecular Biology and Evolution*, *32*, 268–274. https://doi.org/10.1093/molbev/msu300

O'Leary, N. A., Wright, M. W., Brister, J. R., Ciufo, S., Haddad, D., McVeigh, R., Rajput, B., Robbertse, B., Smith-White, B., Ako-Adjei, D., Astashyn, A., Badretdin, A., Bao, Y., Blinkova, O., Brover, V., Chetvernin, V., Choi, J., Cox, E., Ermolaeva, O., … Pruitt, K. D. (2016). Reference sequence (RefSeq) database at NCBI: Current status, taxonomic expansion, and functional annotation. *Nucleic Acids Research*, *44*(D1), D733–D745. https://doi.org/10.1093/nar/gkv1189

Osburn, M. R., LaRowe, D. E., Momper, L. M., & Amend, J. P. (2014). Chemolithotrophy in the continental deep subsurface: Sanford underground research facility (SURF), USA. *Frontiers in Microbiology*, *5*, 1–14. https://doi.org/10.3389/fmicb.2014.00610

Osburn, M. R., Kruger, B., Masterson, A. L., Casar, C. P., & Amend, J. P. (2019). Establishment of the Deep Mine Microbial Observatory (DeMMO), South Dakota, USA, a geochemically stable portal into the deep subsurface. *Frontiers in Earth Science*, *7*, 1–17. https://doi.org/10.3389/feart.2019.00196

Parks, D. H., Rinke, C., Chuvochina, M., Chaumeil, P.-A., Woodcroft, B. J., Evans, P. N., Hugenholtz, P., & Tyson, G. W. (2017). Recovery of nearly 8,000 metagenome-assembled genomes substantially expands the tree of life. *Nature Microbiology*, *2*(11), 1533–1542. https://doi.org/10.1038/s41564-017-0012-7

Philippot, L. (2002). Denitrifying genes in bacterial and Archaeal genomes. *Biochimica et Biophysica Acta (BBA)—Gene Structure and Expression*, *1577*(3), 355–376. https://doi.org/10.1016/S0167-4781(02)00420-7

Potter, S. C., Luciani, A., Eddy, S. R., Park, Y., Lopez, R., & Finn, R. D. (2018). HMMER web server: 2018 update. *Nucleic Acids Research*, *46*(W1), W200–W204. https://doi.org/10.1093/nar/gky448

Priemé, A., Braker, G., & Tiedje, J. M. (2002). Diversity of nitrite reductase (nirK and nirS) gene fragments in forested upland and wetland soils. *Applied and Environmental Microbiology*, *68*(4), 1893–1900. https://doi.org/10.1128/AEM.68.4.1893-1900.2002

Rinaldo, S., Giardina, G., Castiglione, N., Stelitano, V., & Cutruzzolà, F. (2011). The catalytic mechanism of *Pseudomonas aeruginosa* cd1 nitrite reductase. *Biochemical Society Transactions*, *39*(1), 195–200. https://doi.org/10.1042/BST0390195

Roco, C. A., Bergaust, L. L., Bakken, L. R., Yavitt, J. B., & Shapleigh, J. P. (2017). Modularity of nitrogen-oxide reducing soil bacteria: Linking phenotype to genotype. *Environmental Microbiology*, *19*(6), 2507–2519. https://doi.org/10.1111/1462-2920.13250

Sánchez, C., Cabrera, J. J., Gates, A. J., Bedmar, E. J., Richardson, D. J., & Delgado, M. J. (2011). Nitric oxide detoxification in the rhizobia-legume symbiosis. *Biochemical Society Transactions*, *39*(1), 184–188. https://doi.org/10.1042/BST0390184

Sanford, R. A., Wagner, D. D., Wu, Q., Chee-Sanford, J. C., Thomas, S. H., Cruz-García, C., Rodríguez, G., Massol-Deyá, A., Krishnani, K. K., Ritalahti, K. M., Nissen, S., Konstantinidis, K. T., & Löffler, F. E. (2012). Unexpected nondenitrifier nitrous oxide reductase gene diversity and abundance in soils. *Proceedings of the National Academy of Sciences of the United States of America*, *109*(48), 19709–19714. https://doi.org/10.1073/pnas.1211238109

Shiro, Y. (2012). Structure and function of bacterial nitric oxide reductases. *Biochimica et Biophysica Acta (BBA) - Bioenergetics*, *1817*(10), 1907–1913. http://doi.org/10.1016/j.bbabio.2012.03.001

Sievert, S. M., Scott, K. M., Klotz, M. G., Chain, P. S., Hauser, L. J., Hemp, J., Hügler, M., Land, M., Lapidus, A., Larimer, F. W., Lucas, S., Malfatti, S. A., Meyer, F., Paulsen, I. T., Ren, Q., Simon, J., & USF Genomics Class (2008). Genome of the epsilonproteobacterial chemolithoautotroph *Sulfurimonas denitrificans*. *Applied and Environmental Microbiology*, *74*(4), 1145–1156. https://doi.org/10.1128/AEM.01844-07

Spieck, E., Spohn, M., Wendt, K., Bock, E., Shively, J., Frank, J., Indenbirken, D., Alawi, M., Lücker, S., & Hüpeden, J. (2020). Extremophilic nitrite-oxidizing Chloroflexi from Yellowstone hot springs. *ISME Journal*, *14*, 364–379. https://doi.org/10.1038/s41396-019-0530-9

Stein, L. Y., Arp, D. J., Berube, P. M., Chain, P. S., Hauser, L., Jetten, M. S., Klotz, M. G., Larimer, F. W., Norton, J. M., Op den Camp, H. J., Shin, M., & Wei, X. (2007). Whole-genome analysis of the ammonia-oxidizing bacterium, *Nitrosomonas eutropha* C91: Implications for niche adaptation. *Environmental Microbiology*, *9*(12), 2993–3007. https://doi.org/10.1111/j.1462-2920.2007.01409.x

Suharti, Strampraad, M. J. F., Schröder, I., & de Vries, S. (2001). A novel copper A containing menaquinol NO reductase from *Bacillus azotoformans*. *Biochemistry*, *40*(8), 2632–2639. http://doi.org/10.1021/bi0020067

The PyMOL Molecular Graphics System Schrödinger, LLC.

Tria, F. D. K., Landan, G., & Dagan, T. (2017). Phylogenetic rooting using minimal ancestor deviation. *Nature Ecology & Evolution*, *1*, 193. https://doi.org/10.1038/s41559-017-0193

Ward, L. M., Hemp, J., Shih, P. M., McGlynn, S. E., & Fischer, W. W. (2018). Evolution of phototrophy in the Chloroflexi phylum driven by horizontal gene transfer. *Frontiers in Microbiology*, *9*, 1. https://doi.org/10.3389/fmicb.2018.00260

Ward, L. M., McGlynn, S. E., & Fischer, W. W. (2018). Draft genome sequence of a divergent anaerobic member of the Chloroflexi class Ardenticatenia from a sulfidic hot spring. *Genome Announcements*, *6*(25), 1–2. https://doi.org/10.1128/genomeA.00571-18

Waterhouse, A., Bertoni, M., Bienert, S., Studer, G., Tauriello, G., Gumienny, R., Heer, F. T., de Beer, T., Rempfer, C., Bordoli, L., Lepore, R., & Schwede, T. (2018). SWISS-MODEL: Homology modelling of protein structures and complexes. *Nucleic Acids Research*, *46*, W296–W303. https://doi.org/10.1093/nar/gky427

Waterhouse, A. M., Procter, J. B., Martin, D. M., Clamp, M., & Barton, G. J. (2009). Jalview Version 2-A multiple sequence alignment editor and analysis workbench. *Bioinformatics*, *25*, 1189–1191. https://doi.org/10.1093/bioinformatics/btp033

Wei, W., Isobe, K., Nishizawa, T., Zhu, L., Shiratori, Y., Ohte, N., Koba, K., Otsuka, S., & Senoo, K. (2015). Higher diversity and abundance of denitrifying microorganisms in environments than considered previously. *ISME Journal*, *9*(9), 1954–1965. https://doi.org/10.1038/ismej.2015.9

Wu, M., & Scott, A. J. (2012). Phylogenomic analysis of bacterial and archaeal sequences with AMPHORA2. *Bioinformatics*, *28*, 1033–1034. https://doi.org/10.1093/bioinformatics/bts079

Zumft, W. G. (1997). Cell biology and molecular basis of denitrification. *Microbiology and Molecular Biology Reviews*, *61*(4), 533–616. https://doi.org/10.1016/j.sbspro.2014.08.122

Zumft, W. G. (2005). Nitric oxide reductases of prokaryotes with emphasis on the respiratory, heme-copper oxidase type. *Journal of Inorganic Biochemistry*, *99*(1), 194–215. https://doi.org/10.1016/j.jinorgbio.2004.09.024

How to cite this article: Schwartz, S. L., Momper, L., Rangel, L. T., Magnabosco, C., Amend, J. P., & Fournier, G. P. (2022). Novel nitrite reductase domain structure suggests a chimeric denitrification repertoire in the phylum Chloroflexi. *MicrobiologyOpen*, 11, e1258. https://doi.org/10.1002/mbo3.1258

APPENDIX 1

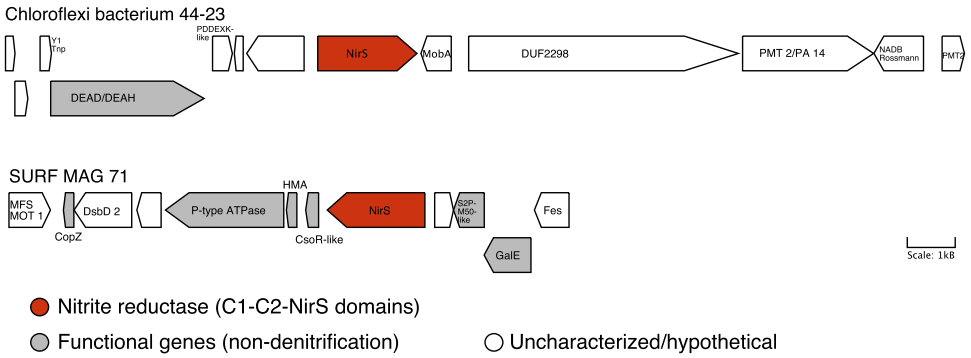

FIGURE A1 C1-C2-NirS gene neighborhoods in Chloroflexi. A gene neighborhood showing the 20,000 base pair region adjacent to the putative nitrite reductase gene containing the C1-C2-NirS domain architecture. Neighborhoods are shown for homologs in Chloroflexi bacterium 44-23 (GenBank accession OJX39483.1) and SURF MAG 71 (GenBank accession RJP52528.1). Expanded descriptions of gene names and functions are provided in Table A2

FIGURE A2 Expanded C2 domain tree. Phylogenetic analysis of C2 domain homologs places the Chloroflexi within a diverse polyphyletic clade including Epsilonproteobacteria, Aquificae, Bacteroidetes, and Planctomycetes; this clade is sister to a broad radiation of Proteobacteria. Support values for selected bipartitions are labeled (aLRT/bb). Support for other nodes is indicated with the following color scheme: Strong support with both values ≥90 (black); weak support with both values ≤50 (white); intermediate support with one or both values between 50 and 90 (gray); conflicting support, with one value ≤50 and the other ≥90 (gray)

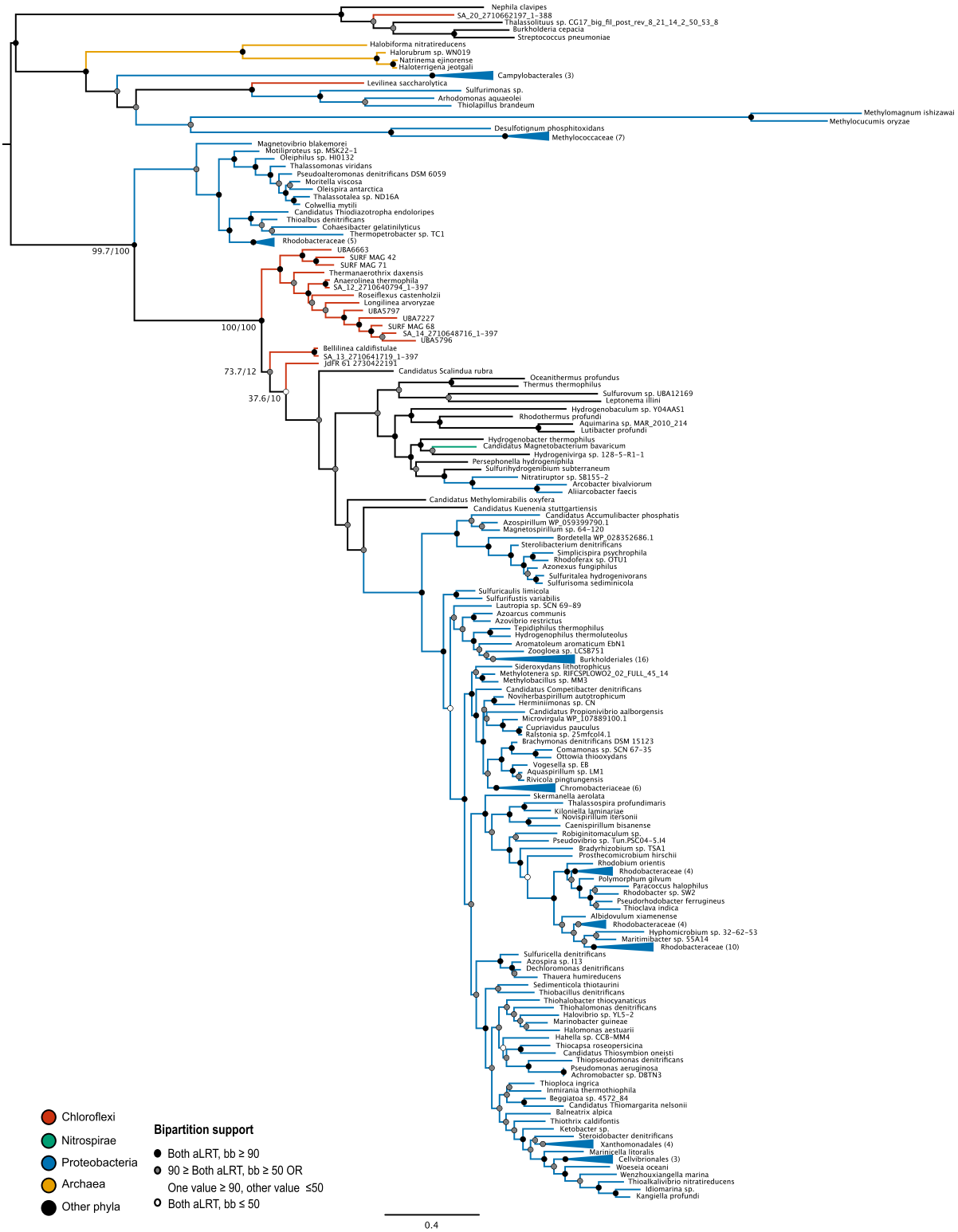

FIGURE A3 Expanded NirS domain tree. Phylogenetic analysis of NirS domain homologs places the Chloroflexi within a polyphyletic clade dominated by Alpha-, Beta-, and Gammaproteobacteria. Support values for selected bipartitions are labeled (aLRT/bb). Support for other nodes is indicated with the following color scheme: Strong support with both values ≥90 (black); weak support with both values ≤50 (white); intermediate support with one or both values between 50 and 90 (gray); conflicting support, with one value ≤50 and the other ≥90 (gray)

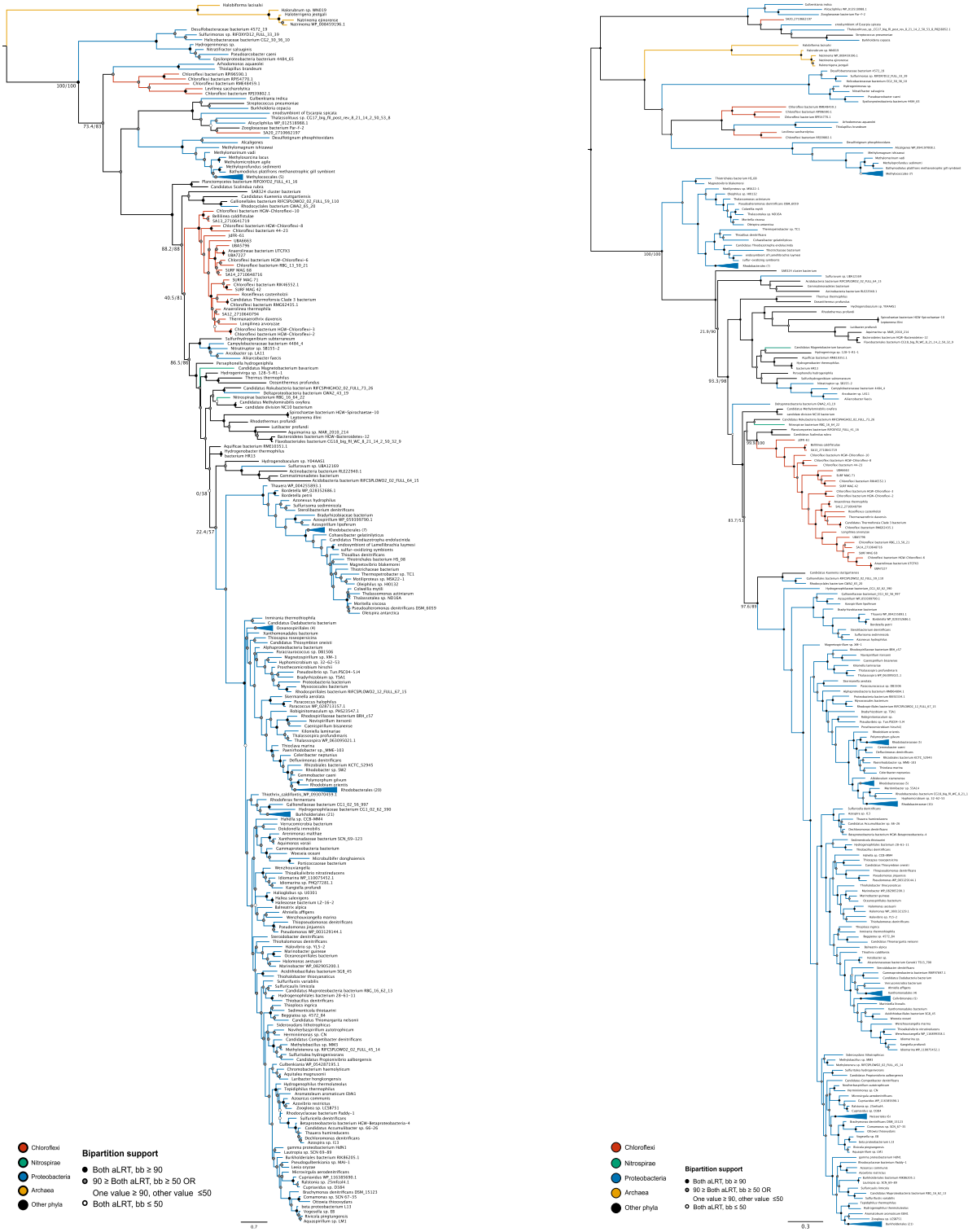

FIGURE A4 Subsampled C2 domain tree. Phylogenetic analysis of C2 domain homologs, subsampled to contain only taxa with both C2 and NirS domains in the nitrite reductase ORF, places the largest clade of Chloroflexi as sister to a polyphyletic group including a large group of Alpha-, Beta-, and Gammaproteobacteria. Support values for selected bipartitions are labeled (aLRT/bb). Support for other nodes is indicated with the following color scheme: Strong support with both values ≥90 (black); weak support with both values ≤50 (white); intermediate support with one or both values between 50 and 90 (gray); conflicting support, with one value ≤50 and the other ≥90 (gray). ORF, open reading frame

FIGURE A5 Subsampled NirS domain tree. Phylogenetic analysis of NirS domain homologs, subsampled to contain only taxa with both C2 and NirS domains in the nitrite reductase ORF, places the largest clade of Chloroflexi as sister to a large radiation of Proteobacteria; these groups are nested within a diverse polyphyletic group. Support values for selected bipartitions are labeled (aLRT/bb). Support for other nodes is indicated with the following color scheme: Strong support with both values ≥90 (black); weak support with both values ≤50 (white); intermediate support with one or both values between 50 and 90 (gray); conflicting support, with one value ≤50 and the other ≥90 (gray). ORF, open reading frame

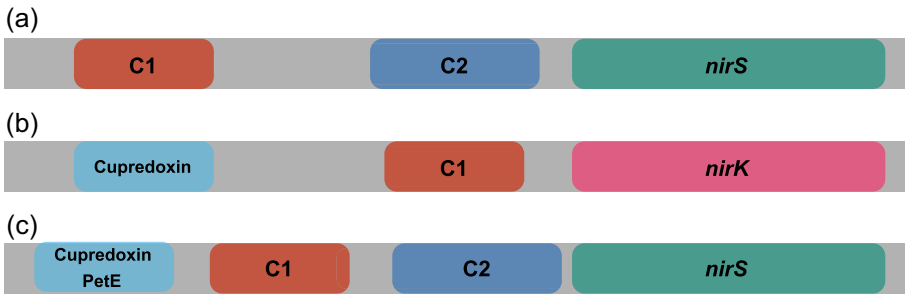

nir architecture	*Examples*
A	SURF MAG 42 (Ga0104751_10026579); UBA5796 (DIDQ01000096.1); Anaerolinea thermophila (WP_013561145.1); Thermanaerothrix daxensis (WP_054521542.1); Longilinea arvoryzae (WP_075072401.1); Bellilinea caldifistulae (WP_082148881.1); Roseiflexus castenholzii (WP_012121904.1)
B	UBA2323 (DDVB01000085.1_15); UBA2356 (DDTU01000029.1_20); UBA2395 (DDSH01000031.1_54); UBA2414 (DDRO01000006.1_183)
C	UBA7227 (DKTP01000143.1_3); uncultured Chloroflexi bacterium (BAL57500.1); SURF MAG 68 (Ga0104751_100097911)

FIGURE A6 Various nitrite reductase architectures within Chloroflexi. Three different open reading frame types including a C1 cytochrome and a nitrite reductase domain appear in surveyed Chloroflexi. The most commonly seen gene features C1, C2, and cytochrome-dependent *nirS* (a); however, C1 is also seen in ORFs with cupredoxin and copper-dependent nitrite reductase (*nirK*) domains (b). A limited number of Chloroflexi genomes also contain ORFs placing C1, C2, and *nirS* together with an N-terminal cupredoxin, plastocyanin (PetE), or similar copper-containing domain (c). ORF, open reading frame

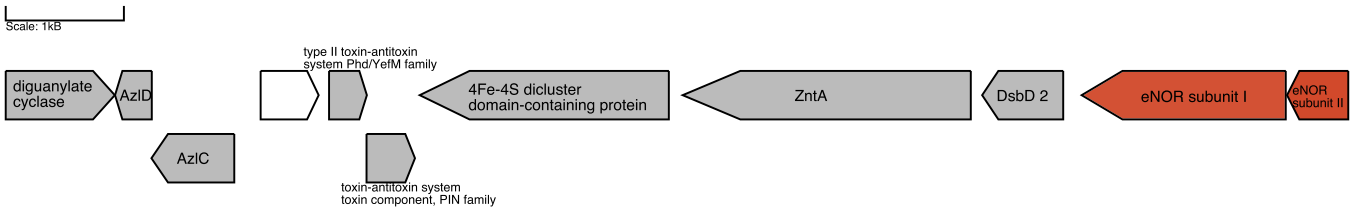

FIGURE A7 eNOR subunit gene neighborhood. A gene neighborhood showing the 20,000 base pair region adjacent to eNOR subunits in SURF MAG 42. Sequence analysis of subunit I (NCBI protein accession RJP50323.1) reflects a conserved glutamine substitution characteristic of the eNOR subfamily. Both proposed subunits of eNOR—the heme-copper cytochrome-containing subunit I, and the cupredoxin-containing subunit II—appear in the MAG. No other denitrification genes appear in the neighborhood. MAG, metagenome-assembled genome; NCBI, National Center for Biotechnology Information; SURF, Sanford Underground Research Facility

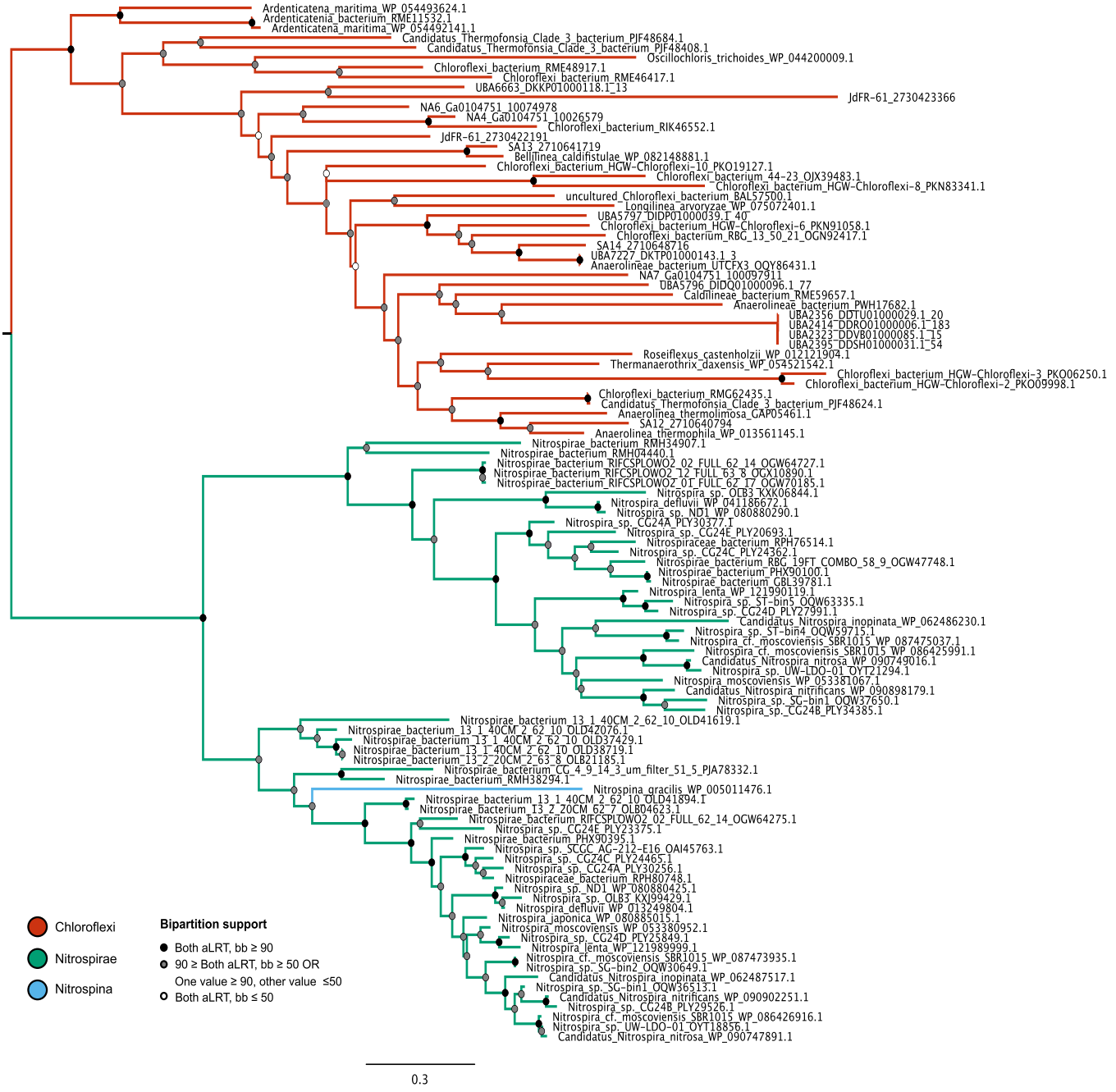

FIGURE A8 Preliminary C1 domain tree. A preliminary phylogenetic tree for C1, including only sequences with $E \leq 10^{-10}$, contains very few overall taxa. The tree contains only members of the Chloroflexi, members of the Nitrospirae, and *Nitrospina gracilis*; the sampling depth does not recover an outgroup for these sister groups. Support for bipartitions is indicated with the following color scheme: Strong support with both values ≥90 (black); weak support with both values ≤50 (white); intermediate support with one or both values between 50 and 90 (gray); conflicting support, with one value ≤50 and the other ≥90 (gray)

APPENDIX 2

TABLE A1 Open reading frame descriptions for SURF MAG 42, *Pseudomonas aeruginosa* PAO1, and *Anaerolinea thermolimosa* NirS gene neighborhoods

Displayed ORF name	Expanded description	Protein ID	Source MAG/organism
Xylose isomerase-like	Sugar phosphate isomerase/epimerase, xylose isomerase-like TIM barrel	RJP53741.1	SURF MAG 42
LuxS	S-ribosylhomocysteine lyase	RJP53742.1	SURF MAG 42
EEVS	2-Epi-5-epi-valiolone synthase/iron-containing alcohol dehydrogenase	RJP53743.1	SURF MAG 42
UbiG	Ubiquinone biosynthesis *O*-methyltransferase/bifunctional 2-polyprenol-6-hydroxyphenol	RJP53744.1	SURF MAG 42
UbiA	ubiA family prenyltransferase	RJP53745.1	SURF MAG 42
MhpC	Alpha/beta hydrolase/pimeloyl-ACP methyl ester carboxylesterase	RJP53746.1	SURF MAG 42
UDG-like	Uracil-DNA glycosylase	RJP53748.1	SURF MAG 42
BaeS	HAMP domain-containing protein/signal transduction kinase	RJP53750.1	SURF MAG 42
N-acetyltransferase	GNAT family *N*-acetyltransferase	RJP53751.1	SURF MAG 42
PrSA	Ribose-phosphate pyrophosphokinase/ phosphoribosylpyrophosphate synthetase	RJP53766.1	SURF MAG 42
PolX	DNA polymerase/3′–5′ exonuclease	RJP53755.1	SURF MAG 42
YdcZ	DMT family transporter	RJP53756.1	SURF MAG 42
Putative PMT 2 superfamily	Dolichyl-phosphate-mannose-protein mannosyltransferase	RJP53757.1	SURF MAG 42
Acetyl-CoA dehydrogenase	Probable acyl-CoA dehydrogenase	AAG03897.1	PAO1
nirN	Probable c-type cytochrome	AAG03898.1	PAO1
SUMT	Probably uroporphyrin-III c-methyltransferase	AAG03899.1	PAO1
nirJ	Heme d1 biosynthesis protein NirJ	AAG03900.1	PAO1
nirH	Heme d1 biosynthesis protein NirH	AAG03901.1	PAO1
nirG	Heme d1 biosynthesis protein NirG/probable transcriptional regulator	AAG03902.1	PAO1
nirL	Heme d1 biosynthesis protein NirL	AAG03903.1	PAO1
nirD	Heme d1 biosynthesis protein nirD/probable transcriptional regulator	AAG03904.1	PAO1
nirF	Heme d1 biosynthesis protein NirF	AAG03905.1	PAO1
nirC	Probable c-type cytochrome precursor	AAG03906.1	PAO1
nirM	Cytochrome c-551 precursor	AAG03907.1	PAO1
nirQ	Regulatory protein NirQ	AAG03909.1	PAO1
Heme-Cu oxidase III	Heme–copper oxidase, subunit III	AAG03911.1	PAO1
norC	Nitric-oxide reductase subunit C	AAG03912.1	PAO1
norB	Nitric-oxide reductase subunit B	AAG03913.1	PAO1
norD	Probable denitrification protein NorD	AAG03914.1	PAO1
Dnr	Transcriptional regulator DNR	AAG03916.1	PAO1
rsmY	Regulatory RNA RsmY/probable transcriptional regulator	AAG03917.1	PAO1

(Continues)

TABLE A1 (Continued)

Displayed ORF name	Expanded description	Protein ID	Source MAG/organism
CynR	Provisional; DNA-binding transcriptional regulator	AAG03917.1	PAO1
YiiM	Uncharacterized conserved protein/MOSC (molybdenum cofactor sulfurase C-terminal)domain-containing protein	AAG03918.1	PAO1
ArgD	Acetylornithine/succinyldiaminopimelate/putrescin e aminotransferase	AAG03919.1	PAO1
TrpB-like	TrpB-like pyridoxal-phosphate dependent enzyme	GAP05449.1	*Anaerolinea thermolimosa*
Gph	Phosphoglycolate phosphatase; haloacid dehalogenase family hydrolase	GAP05450.1	*Anaerolinea thermolimosa*
DR1245-like	Uncharacterized, YbjN domain-containing protein; possible type III secretion system chaperone protein	GAP05451.1	*Anaerolinea thermolimosa*
peptidase C39-like	Peptidase C39-like and TPR domain-containing protein	GAP05452.1	*Anaerolinea thermolimosa*
DUF2568	Hypothetical protein; YrdB family; DUF2568	GAP05453.1	*Anaerolinea thermolimosa*
DUF4388	Hypothetical protein; DUF4388	GAP05454.1	*Anaerolinea thermolimosa*
Srp102	ATP/GTP-binding protein; GTPase, signal recognition particle receptor subunit beta	GAP05455.1	*Anaerolinea thermolimosa*
MhpC	Predicted alpha/beta hydrolase; pimeloyl-ACP methyl ester carboxylesterase	GAP05456.1	*Anaerolinea thermolimosa*
glmU	*N*-acetylglucosamine-1-phosphate uridyltransferase; left-handed parallel beta-helix domain	GAP05458.1	*Anaerolinea thermolimosa*
Cytochrome cd1	Protein containing cytochrome D1 heme domain; nitrite reductase	GAP05460.1	*Anaerolinea thermolimosa*
Cytidylate kinase-like	Cytidylate kinase-like family protein; NK superfamily	GAP05462.1	*Anaerolinea thermolimosa*
Glycosyl hydrolase catalytic core	Glycosyl hydrolases superfamily	GAP05463.1	*Anaerolinea thermolimosa*
Protoheme IX farnesyltransferase	Provisional protoheme IX farnesyltransferase; cytochrome oxidase assembly protein superfamily	GAP05464.1	*Anaerolinea thermolimosa*
SURF1	SURF1 superfamily; similar to yeast cytochrome oxidase assembly protein SHY1	GAP05465.1	*Anaerolinea thermolimosa*
SCO	SCO1/SenC/PrrC; synthesis of cytochrome c oxidase family	GAP05467.1	*Anaerolinea thermolimosa*
Heme Cu oxidase III	Heme–copper oxidase subunit III	GAP05468.1	*Anaerolinea thermolimosa*
COX4 pro	Cytochrome *c* oxidase subunit IV family protein; prokaryotic cytochrome C oxidase subunit IV	GAP05469.1	*Anaerolinea thermolimosa*
Heme Cu oxidase I	Heme–copper oxidase subunit I	GAP05470.1	*Anaerolinea thermolimosa*
CyoA	Cytochrome *c* oxidase, subunit II; cytochrome *c*	GAP05471.1	*Anaerolinea thermolimosa*

Abbreviations: MAG, metagenome-assembled genome; SURF, Sanford Underground Research Facility.

TABLE A2 Open reading frame (ORF) descriptions for Chloroflexi bacterium 44-23 and SURF MAG 71 NirS gene neighborhoods

Displayed ORF name	Expanded description	Protein ID	Source organism
Y1 Tnp	Hypothetical protein; Y1 Tnp superfamily, transposase IS200-like	OJX39478.1	Chloroflexi bacterium 44-23
DEAD/DEAH	DEAD/DEAH box helicase; type I restriction endonuclease subunit R	OJX39479.1	Chloroflexi bacterium 44-23
PDDEXK-like	Hypothetical protein; PDDEXK nuclease-like superfamily	OJX39480.1	Chloroflexi bacterium 44-23
MobA	Hypothetical molybdenum cofactor guanylyltransferase	OJX39484.1	Chloroflexi bacterium 44-23
DUF2298	Hypothetical protein; uncharacterized membrane protein DUF2298 superfamily; helix-hairpin-helix motif	OJX39485.1	Chloroflexi bacterium 44-23
PMT2/PA14	Hypothetical protein; PA14 domain; Dolichyl-phosphate-mannose-protein mannosyltransferase superfamily	OJX39484.1	Chloroflexi bacterium 44-23
NADB Rossmann	Hypothetical protein; NADB Rossmann superfamily; Rossmann-fold NAD(P)(+)-binding proteins	OJX39487.1	Chloroflexi bacterium 44-23
PMT2	Hypothetical protein; Dolichyl-phosphate-mannose-protein mannosyltransferase	OJX39488.1	Chloroflexi bacterium 44-23
MFS MOT1	Hypothetical protein; putative sulfate/molybdate transporter, MFS superfamily	RJP52521.1	SURF MAG 71
CopZ	Copper chaperone CopZ; heavy-metal-associated domain-containing protein	RJP52522.1	SURF MAG 71
DsbD 2	Hypothetical protein; DsbD 2 cytochrome c biogenesis protein transmembrane region; cupredoxin superfamily-containing protein	RJP52523.1	SURF MAG 71
P-type ATPase	Heavy metal translocating P-type ATPase, Cu-like	RJP52525.1	SURF MAG 71
HMA	Heavy metal transporter, HMA superfamily	RJP52526.1	SURF MAG 71
CsoR-like	Metal-sensitive transcriptional regulator; TthCsoR-like DUF156	RJP52527.1	SURF MAG 71
S2P-M50-like	Site-2 protease family protein; zinc metalloproteases	RJP52530.1	SURF MAG 71
GalE	UDP-glucose 4-epimerase; NADB Rossmann superfamily	RJP52531.1	SURF MAG 71
Fes	Hypothetical protein; Fes superfamily; Enterochelin esterase or related enzyme	RJP52532.1	SURF MAG 71

Abbreviations: MAG, metagenome-assembled genome; SURF, Sanford Underground Research Facility.

TABLE A3 Domain families in ORFs with C1 domain homolog but no NirS domain homolog

Domain name	Brief description	Accession(s)
CyoA	Cytochrome/quinol oxidase	RME74748.1
COX IV	Prokaryotic cytochrome c subunit IV	PKB63614.1; PIQ26724.1
tynA	Primary-amine oxidase	WP_095041976.1
CxxCH_TIGR02603	Putative heme-binding domain	WP_095041976.1; OUC09162.1; OGW07928.1; OGP31126.1; OGV95443.1; OGP47454.1; OGP11994.1; OG149337.1; OYT21294.1; OLD38719.1; OLB21185.1
Cupredoxin	N/A	UBA5757_DIDP01000039.1_40
Caa3_CtaG	Cytochrome c oxidase caa3 assembly factor	PYQ29527.1
PRK10856	Cytoskeleton protein RodZ	OQY877.1

(Continues)

TABLE A3 (Continued)

Domain name	Brief description	Accession(s)
EnvC	Septal ring factor, activator of murein hydrolases	RMF78192.1
PRK03735	Provisional cytochrome b6	RME88945.1
DMSOR_beta-like	DMSO reductase beta subunit	RME88945.1
FlpD	Methyl-viologen-reducing hydrogenase, beta subunit	RME88945.1
TTQ_mauG	tryptophan tryptophylquinone biosynthesis enzyme MauG	RIK95915.1
Heme_Cu_Oxidase_I	Heme-copper oxidase subunit I	WP_073101466.1
PRK14486	Putative bifunctional cbb3-type cytochrome c oxidase subunit II	OYW96265.1
YccC	Uncharacterized membrane protein	OLB04623.1; OAI45763.1; WP_080880425.1; KXJ99429.1
FTR1	Iron permease	WP_053380952.1
EcfT	T component of ECF-type transporters	WP_090902251.1
ArsB_NhaD_permease	Anion permease	OYT18856.1; WP_090747891.1

Abbreviation: ORF, open reading frame.

TABLE A4 Heme–copper superfamily active site (modified from Hemp & Gennis, 2008)

Enzyme	Active-site residue	Predicted no. of proton channels	Present in
Oxygen reductase	Y	0–2	All domains; varies by enzyme subfamily
cNOR	E	0	Proteobacteria (Shiro, 2012; Hendriks, 2000)
qNOR	E	0	Proteobacteria, Cyanobacteria, Firmicutes, Archaea (Shiro, 2012; Hemp & Gennis, 2008; Heylen et al., 2007; Hendriks et al, 2000)
sNOR	N	0	Betaproteobacteria, *Silicibacter*, *Deinococcus*, *Geobacillus* (Stein et al., 2007)
eNOR	Q	1	Archaea (Hemp & Gennis, 2008, this study), Chloroflexi (Ward, McGlynn et al., 2018 this study), Proteobacteria (this study)
gNOR	D	0	*Sulfurimonas*, *Sulfurovum*, *Persephonella* (Sievert et al., 2008)
CuANor	N	1	*Bacillus* (Al-Attar & De Vries, 2015; Suharti et al., 2001)

Abbreviations: cNOR, cytochrome-type nitric oxide reductase; qNOR, quinol-dependent nitric oxide reductases.

TABLE A5 MAG source data

Genome	BioProject	BioSample	MAG name	MAG/hit db filename	Publication
1	PRJNA355136	SAMN08499021	SURF MAG 27	NA1	Momper, Jungbluth et al. (2017)
2	PRJNA355136	SAMN08499024	SURF MAG 30	NA2	Momper, Jungbluth et al. (2017
3	PRJNA355136	SAMN08499034	SURF MAG 40	NA3	Momper, Jungbluth et al. (2017)
4[a]	PRJNA355136	SAMN08499036	SURF MAG 42	NA4	Momper, Jungbluth et al. (2017)
5	PRJNA355136	SAMN08499037	SURF MAG 43	NA5	Momper, Jungbluth et al. (2017)

TABLE A5 (Continued)

Genome	BioProject	BioSample	MAG name	MAG/hit db filename	Publication
6	PRJNA355136	SAMN08499065	SURF MAG 71	NA6	Momper, Jungbluth et al. (2017)
7	PRJNA355136	SAMN08499062	SURF MAG 68	NA7	Momper, Jungbluth et al. (2017)
8	PRJNA269163	SAMN06226378	JdFR-61	JdFR61	Jungbluth et al. (2017)
9	PRJNA681409/PRJNA680468	pending release	–	SA8	–
10	PRJNA681409/PRJNA680468	pending release	–	SA9	–
11	PRJNA681409/PRJNA680468	pending release	–	SA10	–
12	PRJNA681409/PRJNA680468	pending release	–	SA11	–
13	PRJNA681409/PRJNA680468	pending release	–	SA12	–
14	PRJNA681409/PRJNA680468	pending release	–	SA13	–
15	PRJNA681409/PRJNA680468	pending release	–	SA14	–
16	PRJNA681409/PRJNA680468	pending release	–	SA15	–
17	PRJNA681409/PRJNA680468	pending release	–	SA16	–
18	PRJNA681409/PRJNA680468	pending release	–	SA17	–
19	PRJNA681409/PRJNA680468	pending release	–	SA18	–
20	PRJNA681409/PRJNA680468	pending release	–	SA19	–
21	PRJNA681409/PRJNA680468	pending release	–	SA20	–

Abbreviations: ORF, open reading frame; MAG, metagenome-assembled genome.

[a]SURF MAG 42 is the source genome for nirS ORF.

TABLE A6 MAG identifying data for sequences selected from Parks et al. (2017)

MAG no.	Organism name		Isolate ID	WGS ID
1	Anaerolineaceae	bacterium	UBA1024	DCER00000000
2	Anaerolineaceae	bacterium	UBA2178	DCVW00000000
3	Anaerolineaceae	bacterium	UBA2274	DDWY00000000
4	Anaerolineaceae	bacterium	UBA6073	DIXT00000000
5	Anaerolineaceae	bacterium	UBA7644	DLIK00000000
6	Anaerolineales	bacterium	UBA1429	DCTX00000000
7	Anaerolineales	bacterium	UBA2181	DCVT00000000
8	Anaerolineales	bacterium	UBA2200	DCVA00000000
9	Anaerolineales	bacterium	UBA2317	DDVH00000000
10	Anaerolineales	bacterium	UBA2323	DDVB00000000
11	Anaerolineales	bacterium	UBA2356	DDTU00000000
12	Anaerolineales	bacterium	UBA2395	DDSH00000000
13	Anaerolineales	bacterium	UBA2414	DDRO00000000
14	Anaerolineales	bacterium	UBA2796	DEHQ00000000
15	Anaerolineales	bacterium	UBA6092	DIXA00000000
16	Anaerolineales	bacterium	UBA6663	DKKP00000000
17	Anaerolineales	bacterium	UBA6665	DKKN00000000
18	Anaerolineales	bacterium	UBA7227	DKTP00000000
19	Chloroflexaceae	bacterium	UBA1466	DCSM00000000

(Continues)

TABLE A6 (Continued)

MAG no.	Organism name		Isolate ID	WGS ID
20	Chloroflexi	bacterium	UBA2235	DDYL00000000
21	Chloroflexi	bacterium	UBA5177	DHWR00000000
22	Chloroflexi	bacterium	UBA5183	DHWL00000000
23	Chloroflexi	bacterium	UBA6042	DIYY00000000
24	Chloroflexi	bacterium	UBA6077	DIXP00000000
25	Chloroflexi	bacterium	UBA6265	DJVD00000000
26	Chloroflexi	bacterium	UBA6622	DJHK00000000
27	Dehalococcoidia	bacterium	UBA1127	DCAS00000000
28	Dehalococcoidia	bacterium	UBA1151	DBZV00000000
29	Dehalococcoidia	bacterium	UBA1222	DBXC00000000
30	Dehalococcoidia	bacterium	UBA2141	DCXH00000000
31	Dehalococcoidia	bacterium	UBA2158	DCWQ00000000
32	Dehalococcoidia	bacterium	UBA2160	DCWO00000000
33	Dehalococcoidia	bacterium	UBA2243	DDYD00000000
34	Dehalococcoidia	bacterium	UBA2247	DDXZ00000000
35	Dehalococcoidia	bacterium	UBA2588	DDKW00000000
36	Dehalococcoidia	bacterium	UBA2768	DEIS00000000
37	Dehalococcoidia	bacterium	UBA2962	DEBG00000000
38	Dehalococcoidia	bacterium	UBA2979	DEAP00000000
39	Dehalococcoidia	bacterium	UBA6234	DJWI00000000
40	Dehalococcoidia	bacterium	UBA6803	DKFF00000000
41	Dehalococcoidia	bacterium	UBA6926	DKAM00000000
42	Dehalococcoidia	bacterium	UBA6951	DJZN00000000
43	Dehalococcoidia	bacterium	UBA6956	DJZI00000000
44	Dehalococcoidia	bacterium	UBA7833	DLTP00000000
45	Dehalococcoidia	bacterium	UBA7894	DLRG00000000
46	Dehalococcoidia	bacterium	UBA826	DBHO00000000
47	bacterium	UBP15	UBA6099	DIWT00000000
48	Anaerolineaceae	bacterium	UBA4775	DHHJ00000000
49	Anaerolineaceae	bacterium	UBA4784	DHHA00000000
50	Anaerolineaceae	bacterium	UBA4841	DHEV00000000
51	Anaerolineaceae	bacterium	UBA4890	DHCY00000000
52	Anaerolineaceae	bacterium	UBA4929	DHBL00000000
53	Anaerolineaceae	bacterium	UBA5199	DHVV00000000
54	Anaerolineaceae	bacterium	UBA5224	DHUW00000000
55	Anaerolineaceae	bacterium	UBA5229	DHUR00000000
56	Anaerolineaceae	bacterium	UBA5241	DHUF00000000
57	Anaerolineaceae	bacterium	UBA5243	DHUD00000000
58	Anaerolineaceae	bacterium	UBA5311	DHRN00000000
59	Anaerolineaceae	bacterium	UBA5344	DHQG00000000

MAG no.	Organism name		Isolate ID	WGS ID
60	Anaerolineaceae	bacterium	UBA5355	DHPV00000000
61	Anaerolineaceae	bacterium	UBA5404	DHNY00000000
62	Anaerolineaceae	bacterium	UBA5823	DICP00000000
63	Anaerolineales	bacterium	UBA4142	DFWE00000000
64	Anaerolineales	bacterium	UBA4826	DHFK00000000
65	Anaerolineales	bacterium	UBA5215	DHVF00000000
66	Anaerolineales	bacterium	UBA5796	DIDQ00000000
67	Anaerolineales	bacterium	UBA5797	DIDP00000000
68	Chloroflexi	bacterium	UBA4669	DHLL00000000
69	Chloroflexi	bacterium	UBA4730	DHJC00000000
70	Chloroflexi	bacterium	UBA4733	DHIZ00000000
71	Chloroflexi	bacterium	UBA4735	DHIX00000000
72	Chloroflexi	bacterium	UBA4736	DHIW00000000
73	Chloroflexi	bacterium	UBA5189	DHWF00000000
74	Chloroflexi	bacterium	UBA6019	DIZV00000000
75	Dehalococcoides	mccartyi	UBA5818	DICU00000000
76	Dehalococcoides	mccartyi	UBA5554	DIMY00000000
77	Dehalococcoides	mccartyi	UBA5545	DINH00000000
78	Dehalococcoides	mccartyi	UBA5853	DJGF00000000
79	Dehalococcoides	mccartyi	UBA5846	DJGM00000000
80	Dehalococcoidia	bacterium	UBA3088	DFBE00000000
81	Dehalococcoidia	bacterium	UBA4086	DFYI00000000
82	Dehalococcoidia	bacterium	UBA4087	DFYH00000000
83	Dehalococcoidia	bacterium	UBA4462	DGOQ00000000
84	Dehalococcoidia	bacterium	UBA5760	DIFA00000000
85	Leptolinea	sp	UBA4782	DHHC00000000
86	Nitrospinaceae	bacterium	UBA3496	DFQF00000000

Abbreviation: MAG, metagenome-assembled genome.

TABLE A7 Model data by domain/gene tree

Gene/ORF	Figure no.	Substitution model (selected by IQ Tree MF)
C1, no outgroup	A8	WAG+F+R4
C1, with outgroup	5	WAG+F+R6
C2	4, A2	LG+R7
NirS	4, A3	LG+F+R7
eNOR	6	LG+F+R6

Abbreviation: ORF, open reading frame.